

---

# Freeze and Chaos for DNNs: an NTK view of Batch Normalization, Checkerboard and Boundary Effects

---

**Arthur Jacot**

Ecole Polytechnique Fédérale de Lausanne  
arthur.jacot@epfl.ch

**Franck Gabriel**

Ecole Polytechnique Fédérale de Lausanne  
franck.gabriel@epfl.ch

**Clément Hongler**

Ecole Polytechnique Fédérale de Lausanne  
clement.hongler@epfl.ch

## Abstract

In this paper, we analyze a number of architectural features of Deep Neural Networks (DNNs), using the so-called Neural Tangent Kernel (NTK). The NTK describes the training trajectory and generalization of DNNs in the infinite-width limit.

In this limit, we show that for (fully-connected) DNNs, as the depth grows, two regimes appear: “freeze” (also known as “order”), where the (scaled) NTK converges to a constant (slowing convergence), and “chaos”, where it converges to a Kronecker delta (limiting generalization).

We show that when using the scaled ReLU as a nonlinearity, we naturally end up in the “freeze”. We show that Batch Normalization (BN) avoids the freeze regime by reducing the importance of the constant mode in the NTK. A similar effect is obtained by normalizing the nonlinearity which moves the network to the chaotic regime.

We uncover the same “freeze” and “chaos” modes in Deep Deconvolutional Networks (DC-NNs). The “freeze” regime is characterized by checkerboard patterns in the image space in addition to the constant modes in input space. Finally, we introduce a new NTK-based parametrization to eliminate border artifacts and we propose a layer-dependent learning rate to improve the convergence of DC-NNs.

We illustrate our findings by training DCGANs using our setup. When trained in the “freeze” regime, we see that the generator collapses to a checkerboard mode. We also demonstrate numerically that the generator collapse can be avoided and that good quality samples can be obtained, by tuning the nonlinearity to reach the “chaos” regime (without using batch normalization).

## 1 Introduction

The training of Deep Neural Networks (DNN) involves a great variety of architecture choices. It is therefore crucial to find tools to understand their effects and to compare them.

For example, Batch Normalization (BN) [11] has proven to be crucial in the training of DNNs but remains ill-understood. While BN was initially introduced to solve the problem of “covariate shift”, recent results [25] suggest an effect on the smoothness of the loss surface. Some alternatives to BN have been proposed [18, 24, 15], yet it remains difficult to compare them theoretically. Recent theoretical results [29] suggest some relation to the transition from “freeze” (also known as “order”) to “chaos” observed as the depth of the NN goes to infinity [22, 6, 28].

The impact of architecture is very apparent in GANs [10]: their results are heavily affected by the architecture of the generator and discriminator [23, 30, 4, 14] and the training may fail without BN [3, 26].

Recently, a number of important advances [12, 7, 1] have allowed one to understand the training of DNNs when the number of neurons in each hidden layer is very large. These new results give new tools to study the asymptotic effect of BN. In particular, the Neural Tangent Kernel (NTK) [12] illustrates the effect of architecture on the training of DNNs and also describes their loss surface [13]. The NTK can easily be extended to CNNs and other architectures [27, 2], hence allowing comparison.

## 1.1 Our Contributions

We describe how the NTK is affected by the “freeze” and “chaos” regimes [22, 6, 28]. For fully-connected networks (FC-NNs), the scaled NTK converges to a constant in the “freeze” regime and to a Kronecker delta in the “chaos” regime. In deconvolutional networks (DC-NNs), a similar transition takes place: the “freeze” regime features checkerboard patterns [20] and the “chaos” regime features a (translation invariant) Kronecker delta.

We then show that different normalization techniques such as Batch Normalization and our proposed Nonlinearity Normalization with hyper-parameter tuning allows the DNN to avoid the “freeze” regime.

Besides, we prove that the traditional parametrization of DC-NNs leads to border effects in the NTK and we propose a simple solution suggesting a new “parent-based” parametrization. At last, the effect of the number of channels on the NTK is discussed, giving a theoretical motivation for decreasing the number of channels after each upsampling. We show that using a layer-dependent learning rate allows to balance the contributions of the layers to the learning.

Finally, we demonstrate our findings numerically on DC-GANs: we show that in the “freeze” regime, the generator collapses to a checkerboard mode. We show how a basic DC-GAN can be effectively trained by avoiding this mode collapse: by proper hyperparameter tuning, nonlinearity normalization, parametrization and learning rate choices, without using batch normalization, we are able to reach the “chaos” regime and to get good quality samples from a very simple DC-NN generator.

## 2 Setup

In this section, we introduce the two architectures that we will consider, FC-NNs and DC-NN, and their training procedures.

### 2.1 Fully-Connected Neural Nets

The first type of architecture we consider are deep Fully-Connected Neural Nets (FC-NNs). An FC-NN  $\mathbb{R}^{n_0} \rightarrow \mathbb{R}^{n_L}$  with nonlinearity  $\sigma : \mathbb{R} \rightarrow \mathbb{R}$  consists of  $L + 1$  layers ( $L - 1$  hidden layers), each containing  $n_0, n_1, \dots, n_L$  neurons. The parameters are defined by connection weight matrices  $W^{(\ell)} \in \mathbb{R}^{n_{\ell+1} \times n_\ell}$  and bias vectors  $b^{(\ell)} \in \mathbb{R}^{n_{\ell+1}}$  for  $\ell = 0, 1, \dots, L - 1$ . Following [12], the network parameters are aggregated into a single vector  $\theta \in \mathbb{R}^P$  and initialized using iid standard Gaussians  $\mathcal{N}(0, 1)$ . For  $\theta \in \mathbb{R}^P$ , the ANN  $f_\theta : \mathbb{R}^{n_0} \rightarrow \mathbb{R}^{n_L}$  is defined as  $f_\theta(x) = \tilde{\alpha}^{(L)}(x)$ , where the activations and preactivations  $\alpha^{(\ell)}, \tilde{\alpha}^{(\ell)}$  are recursively constructed using the NTK parametrization: we set  $\alpha^{(0)}(x) = x$  and, for  $\ell = 0, \dots, L - 1$ ,

$$\tilde{\alpha}^{(\ell+1)}(x) = \frac{\sqrt{1 - \beta^2}}{\sqrt{n_\ell}} W^{(\ell)} \alpha^{(\ell)}(x) + \beta b^{(\ell)}, \quad \alpha^{(\ell+1)}(x) = \sigma\left(\tilde{\alpha}^{(\ell+1)}(x)\right),$$

where  $\sigma$  is applied entry-wise and  $\beta \geq 0$ .

**Remark 1.** *The NTK initialization is equivalent to the so-called Le Cun initialization scheme [16], where each connection weight of the  $\ell$ -th layer is initialized with standard deviation  $\frac{1}{\sqrt{n_\ell}}$ ; in our approach, the  $\frac{1}{\sqrt{n_\ell}}$  appears in the parametrization of the network. While the behavior at initialization is similar, the NTK parametrization ensures that the training is consistent as the size of the layers grows, see [12].*

The hyperparameter  $\beta$  allows one to balance the relative contributions of the connection weights and of the biases during training; in our numerical experiments, we set  $\beta = 0.1$ . Note that the variance of the normalized bias  $\beta b^{(\ell)}$  at initialization can be tuned by  $\beta$ .

## 2.2 Deconvolutional Neural Networks

The second type of architecture we consider are Deconvolutional Nets (DC-NN), also known as Transpose ConvNets or Fractionally Strided ConvNets [8]. A DC-NN in dimension  $d$  with  $L$  layers, channel numbers  $n_\ell$ , windows  $\omega_\ell \subset \mathbb{Z}^d$  and padding windows  $\pi_\ell \subset \omega_\ell$  for  $\ell = 0, \dots, L-1$ , consists of a composition of the following operations:

- The *upsampling*  $v^{(\ell)} : (\mathbb{R}^{n_\ell})^{I_\ell} \rightarrow (\mathbb{R}^{n_\ell})^{\tilde{I}_{\ell+1}}$ , with stride  $s \in \{1, 2, 3, \dots\}^d$ , constructs a ‘blown-up’ image  $(y_q)_{q \in \tilde{I}_{\ell+1}}$  from  $(x_p)_{p \in I_\ell}$  by  $y_q = x_{q/s}$  if  $s \mid q$  (i.e. if for any  $i$ ,  $s_i \mid q_i$ ) and  $y_q = 0$  if not.

- The *DC-filter*  $\gamma^{(\ell)} : (\mathbb{R}^{n_\ell})^{\tilde{I}_{\ell+1}} \rightarrow (\mathbb{R}^{n_{\ell+1}})^{I_{\ell+1}}$  constructs an ‘output’  $(y_q)_{q \in I_{\ell+1}}$  where  $I_{\ell+1} = \cup_{p \in \tilde{I}_{\ell+1}} (p + \pi_\ell)$ , as follows: we define  $y_q \in \mathbb{R}^{n_{\ell+1}}$  by

$$y_q = \frac{\sqrt{1 - \beta^2}}{\sqrt{n_\ell^{|\omega|/s_1 \dots s_d}}} W^{(\ell)}(x_{q+\omega}) + \beta b^{(\ell)},$$

where the matrix  $W^{(\ell)} \in \mathbb{R}^{n_{\ell+1} \times n_\ell^{|\omega|}}$  encodes a linear map,  $b^{(\ell)} \in \mathbb{R}^{n_{\ell+1}}$  and  $|\omega|$  denotes the cardinality of  $\omega$ ; we apply ‘zero-padding’, setting  $x_p = 0 \in \mathbb{R}^{n_\ell}$  for  $p \notin \tilde{I}_{\ell+1}$ .

- The pointwise application of the nonlinearity  $\sigma : \mathbb{R} \rightarrow \mathbb{R}$  (to each channel of each pixel).

The parameters are aggregated into a vector  $\theta \in \mathbb{R}^P$  and initialized as iid standard Gaussians  $\mathcal{N}(0, 1)$ .

For  $\theta \in \mathbb{R}^P$ , the DC-NN  $f_\theta : (\mathbb{R}^{n_0})^{I_0} \rightarrow (\mathbb{R}^{n_L})^{I_L}$  is defined as the composition

$$(\mathbb{R}^{n_0})^{I_0} \xrightarrow{v^{(0)}} (\mathbb{R}^{n_0})^{\tilde{I}_1} \xrightarrow{\gamma^{(0)}} (\mathbb{R}^{n_0})^{I_1} \xrightarrow{\sigma} (\mathbb{R}^{n_0})^{I_1} \xrightarrow{v^{(1)}} \dots \xrightarrow{\sigma} (\mathbb{R}^{n_0})^{I_{L-1}} \xrightarrow{v^{(L)}} (\mathbb{R}^{n_0})^{\tilde{I}_L} \xrightarrow{\gamma^{(L)}} (\mathbb{R}^{n_0})^{I_L}.$$

## 2.3 Training and Setup

In this section, we describe the training of ANNs in the FC-NN case to keep the notation light; the generalization to the DC-NN case is straightforward. For a dataset  $x_1, \dots, x_N \in \mathbb{R}^{n_0}$ , we define the *output* matrix  $Y : \mathbb{R}^P \rightarrow \mathbb{R}^{n_L \times N}$  by  $Y(\theta) = (f_{\theta,k}(x_i))_{1 \leq i \leq N, 1 \leq k \leq n_L}$ . The ANN is trained by optimizing a cost  $C : \mathbb{R}^{n_L \times N} \rightarrow \mathbb{R}$  through gradient descent, defining a flow  $\partial_t \theta_t = -\nabla_\theta C(Y) \big|_{\theta_t}$ .

In this paper, we focus on the so called *over-parametrized regime*, where the sizes of the hidden layers  $n_1, \dots, n_{L-1} \rightarrow \infty$  (either sequentially, as in [12] or simultaneously, as in [27, 2]), for fixed  $L$ . In the case of FC-NNs, this amounts to taking large widths for the hidden layers, while for the DC-NNs, this amounts to taking large channel numbers.

## 3 Neural Tangent Kernel

The Neural Tangent Kernel (NTK) [12] is at the heart of our analysis of the overparametrized regime. It describes the evolution of  $(f_{\theta_t})_{t \geq 0}$  in function space during training. In the FC-NN case, the NTK  $\Theta_\theta^{(L)} : \mathbb{R}^{n_0} \times \mathbb{R}^{n_0} \rightarrow \mathbb{R}^{n_L \times n_L}$  is defined by

$$\Theta_{\theta, k k'}^{(L)}(x, x') = \sum_{p=1}^P \partial_{\theta_p} f_{\theta, k}(x) \partial_{\theta_p} f_{\theta, k'}(x').$$

For a finite dataset  $x_1, \dots, x_N$ , the NTK Gram Matrix  $\tilde{\Theta}_\theta^{(L)} \in \mathbb{R}^{n_L N \times n_L N}$  is defined by  $\tilde{\Theta}_{\theta, ik, jm}^{(L)} = \Theta_{\theta, km}^{(L)}(x_i, x_j)$ . The evolution of  $f_\theta$  can then be written in terms of the NTK as follows

$$\partial_t f_{\theta_t, k}(x) = - \sum_{i=1}^N \sum_{j=1}^{n_L} \Theta_{\theta_t, kj}^{(L)}(x, x_i) \left( \frac{\partial C}{\partial y_{ij}} \right) \bigg|_{Y(\theta_t)}.$$

In the DC-NN case, the NTK  $\Theta_\theta^{(L)} : (\mathbb{R}^{n_0})^{I_0} \times (\mathbb{R}^{n_0})^{I_0} \rightarrow \mathbb{R}^{n_L |I_L| \times n_L |I_L|}$  is defined by a similar formula: the  $n_L \times n_L$  matrix  $\Theta_{\theta, pp'}^{(L)}(x, x')$  represents how a ‘pressure’ to change the pixel  $p$  produced by the ‘code’  $x$  influences the value of the pixel  $p'$  produced by the ‘code’  $x'$ .

### 3.1 Infinite-Width Limit for FC-NNs

Following [19, 5, 17], in the overparametrized regime at initialization, the pre-activations  $(\tilde{\alpha}_i^{(\ell)})_{i=1, \dots, n_\ell}$  are described by iid centered Gaussian processes with covariance kernels  $\Sigma^{(\ell)}$  constructed as follows. For a kernel  $K$ , set

$$\mathbb{L}_K^g(z_0, z_1) = \mathbb{E}_{(y_0, y_1) \sim \mathcal{N}(0, (K(z_i, z_j))_{i, j=0, 1})} [g(y_0) g(y_1)].$$

The activation kernels  $\Sigma^{(\ell)}$  are defined recursively by  $\Sigma^{(0)}(z_0, z_1) = \beta^2 + \frac{(1-\beta^2)}{n_0} z_0^T z_1$  and  $\Sigma^{(\ell+1)} = \beta^2 + (1-\beta^2) \mathbb{L}_{\Sigma^{(\ell)}}^\sigma$ .

While random at initialization, in the infinite-width-limit, the NTK converges to a deterministic limit, which is moreover constant during training:

**Theorem 1.** *As  $n_1, \dots, n_{L-1} \rightarrow \infty$ , for any  $z_0, z_1$  and any  $t \geq 0$ , the kernel  $\Theta_{\theta_t}^{(L)}(z_0, z_1)$  converges to  $\Theta_\infty^{(L)}(z_0, z_1) \otimes \text{Id}_{n_L}$ , where  $\Theta_\infty^{(L)}(z_0, z_1) = \sum_{\ell=1}^L \Sigma^{(\ell)}(z_0, z_1) \prod_{l=\ell+1}^L \dot{\Sigma}^{(l)}(z_0, z_1)$  and  $\dot{\Sigma}^{(l)} = (1-\beta^2) \mathbb{L}_{\Sigma^{(l-1)}}^{\dot{\sigma}}$  with  $\dot{\sigma}$  denoting the derivative of  $\sigma$ .*

[12] gives a proof for the sequential limit  $n_1 \rightarrow \infty, \dots, n_{L-1} \rightarrow \infty$  and [27, 2] a proof in the simultaneous limit  $\min(n_1, \dots, n_{L-1}) \rightarrow \infty$ . As a consequence, in the infinite-width limit, the dynamics of the function  $f_{\theta_t}$  acquires a simple form:

$$\partial_t f_{\theta_t, k}(x) = - \sum_{i=1}^N \Theta_\infty^{(L)}(x, x_i) \left( \frac{\partial C}{\partial y_{ik}} \right) \Bigg|_{Y(\theta_t)}.$$

### 3.2 Infinite-Channel-Number for DC-NNs

The infinite-channel-number limit for DC-NNs follows a similar analysis with the difference that the weights are shared in the architecture. In [27, 2], a number of results have been derived for the initialization and are generalized in our setting in Appendix E. Based on the existing results, it appears naturally to postulate the following:

**Conjecture 1.** *As  $n_1, \dots, n_{L-1} \rightarrow \infty$ , the DC-NN NTK has a deterministic, time-constant limit.*

## 4 Freeze and Chaos: Constant Modes, Checkerboard Artifacts

We now investigate the large  $L$  behavior on the NTK (in the infinite-width limit), revealing a transition between two phases which we call ‘freeze’ and ‘chaos’. We start with a few key definitions:

**Definition 1.** *We say that a Lipschitz nonlinearity  $\sigma$  is standardized if  $\mathbb{E}_{x \sim \mathcal{N}(0, 1)} [\sigma^2(x)] = 1$ . For a standardized  $\sigma$ , we define its characteristic value  $r_{\sigma, \beta}$  as  $(1-\beta^2) \mathbb{E}_{x \sim \mathcal{N}(0, 1)} [\dot{\sigma}^2(x)]$ , where  $\dot{\sigma}$  denotes the (a.e. defined) derivative of  $\sigma$ . We denote by  $\vartheta^{(L)}$  the normalized NTK defined by*

$$\vartheta^{(L)}(x, y) = \Theta_\infty^{(L)}(x, y) / \sqrt{\Theta_\infty^{(L)}(x, x) \Theta_\infty^{(L)}(y, y)} \quad \forall x, y \in \mathbb{R}^{n_0} \text{ (FC-NN case),}$$

$$\vartheta_{pp'}^{(L)}(x, y) = \Theta_{\infty, pp'}^{(L)}(x, y) / \sqrt{\Theta_{\infty, pp'}^{(L)}(x, x) \Theta_{\infty, p'p'}^{(L)}(y, y)} \quad \forall x, y \in (\mathbb{R}^{n_0})^{I_0} \text{ (GCD-NN case).}$$

We define the standard  $\sqrt{n_0}$ -spheres by

$$\begin{aligned} \mathbb{S}_{n_0} &= \{x \in \mathbb{R}^{n_0} : \|x\| = \sqrt{n_0}\}, \\ \mathbb{S}_{n_0}^{I_0} &= \left\{ x \in (\mathbb{R}^{n_0})^{I_0} : \|x_p\| = \sqrt{n_0} \quad \forall p \in I_0 \right\}. \end{aligned}$$

Following [6], we consider standardized nonlinearities and inputs in  $\mathbb{S}_{n_0}$  (and  $\mathbb{S}_{n_0}^{I_0}$  for DC-NNs). This ensures that the variance of the neurons is constant for all depths:  $\Sigma^{(\ell)}(x, x) = 1$ . Our techniques

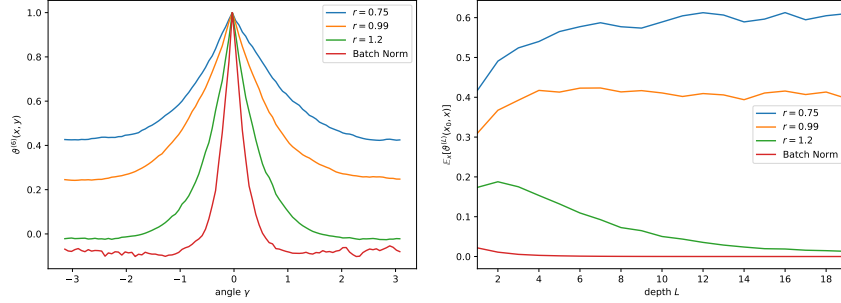


Figure 1: (Left) the NTK on the unit circle for  $L = 6$  and (right) average of the normalized NTK  $\vartheta^{(L)}(x_0, \cdot)$  on the circle as a function of  $L$ . Four architectures are plotted: vanilla ReLU network with  $\beta = 0.5$  (freeze  $r = 0.75$ ) and  $\beta = 0.1$  (edge of chaos  $r = 0.99$ ), with a normalized ReLU (chaos  $r = 1.2$ ) and with Batch Norm.

extend to inputs which have the same norm, as is approximately the case for high dimensional datasets: for example in GANs [10] the inputs of a generator are vectors of iid  $\mathcal{N}(0, 1)$  entries which concentrate around  $\mathbb{S}_{n_0}$  when the dimension  $n_0$  is high.

#### 4.1 Freeze and Chaos for Fully-Connected Networks

For a standardized  $\sigma$ , the large-depth behavior of the NTK is governed by the characteristic value:

**Theorem 2.** *Suppose that  $\sigma$  is twice differentiable and standardized.*

*If  $r_{\sigma, \beta} < 1$ , we are in the frozen regime: there exists  $C_1$  such that for  $x, y \in \mathbb{S}_{n_0}$ ,*

$$1 - C_1 L r_{\sigma, \beta}^L \leq \vartheta^{(L)}(x, y) \leq 1.$$

*If  $r_{\sigma, \beta} > 1$ , we are in the chaotic regime: for  $x \neq \pm y$  in  $\mathbb{S}_{n_0}$ , there exist  $h < 1$  and  $C_2$ , such that*

$$\left| \vartheta^{(L)}(x, y) \right| \leq C_2 h^L.$$

Theorem 2 shows that in the frozen regime, the normalized NTK  $\vartheta^{(L)}$  converges to a constant, whereas in the chaotic regime, it converges to a Kronecker  $\delta$  (taking value 1 on the diagonal, 0 elsewhere). This suggests that the training of deep FC-NN is heavily influenced by the characteristic value  $r_{\sigma, \beta}$ : when  $r_{\sigma, \beta} < 1$ ,  $\Theta^{(L)}$  becomes constant, thus slowing down the training, whereas when  $r_{\sigma, \beta} > 1$ ,  $\Theta^{(L)}$  is concentrates on the diagonal, ensuring fast training, but limiting generalization. To train very deep FC-NNs, it is best to lie “on the edge of chaos”  $r_{\sigma, \beta} = 1$  [22, 28]. When the depth is not too large, it appears possible to lean into the chaotic regime to speed up training without sacrificing generalization.

The standardized ReLU  $\sigma(x) = \sqrt{2} \max(x, 0)$ , has characteristic value  $r_{\sigma, \beta} = 1 - \beta^2$ , which lies in the frozen regime for  $\beta > 0$ . The non-differentiability of  $\sigma$  leads to a different behavior as  $L$  grows:

**Theorem 3.** *With the same notation as in Theorem 2, taking  $\sigma$  to be the standardized ReLU and  $\beta > 0$ , we are in the weakly frozen regime: there exists a constant  $C$  such that  $1 - C r_{\sigma, \beta}^{L/2} \leq \vartheta^{(L)}(x, y) \leq 1$ .*

When  $\beta = 0.1$  the characteristic value  $r$  is equal to 0.99, which is very close to the transition between the two regimes. To really lie in the freeze regime, we require a larger  $\beta$ . In Figure 1, we see that even at the edge of chaos, a ReLU Net with  $\beta = 0.1$  has a strong affinity to the constant mode as witnessed by the large average value of the normalized NTK on the circle  $\mathbb{E}_x [\vartheta^{(L)}(x_0, x)]$ , for  $x_0$  a fixed point of  $\mathbb{S}_{n_0}$  and  $x$  sampled uniformly on  $\mathbb{S}_{n_0}$ . In Section 5, we present a normalization technique to reach the chaotic regime with a ReLU Net.

#### 4.2 Bulk Freeze and Chaos for Deconvolutional Nets

For DC-NNs, the value of an output neuron at a position  $p \in I_L$  only depends on the inputs which are ancestors of  $p$ , i.e. all positions  $q \in I_0$  such that there is a chain of connections from  $q$  to  $p$ . For

the same reason, the NTK  $\Theta_{p,p'}^{(L)}(x, y)$  only depends on the values  $x_q, y_{q'}$  for  $q, q' \in I_0$  ancestors of  $p$  and  $p'$  respectively.

For a stride  $s \in \{2, 3, \dots\}^d$ , we denote the  $s$ -valuation  $v_s(n)$  of  $n \in \mathbb{Z}^d$  as the largest  $k \in \{0, 1, 2, \dots\}$  such that  $s_i^k \mid n_i$  for all  $i = 1, \dots, d$ . The behaviour of the NTK  $\Theta_{p,p'}^{(L)}(x, y)$  depends on the  $s$ -valuation  $v = v_s(p' - p)$  of the difference of the two output positions. If  $v$  is strictly smaller than  $L$ , the NTK  $\Theta_{p,p'}^{(L)}(x, y)$  converges to a constant in the infinite-width limit for any  $x, y \in \mathbb{S}_{n_0}^{I_0}$ .

Again the characteristic number  $r_{\sigma,\beta}$  plays a central role in the behavior of the large-depth limit.

**Theorem 4.** *Take  $I_0 = \mathbb{Z}^d$ , and consider a DC-NN with upsampling stride  $s \in \{2, 3, \dots\}^d$ , windows  $\pi_\ell = \omega_\ell = \{0, \dots, w_1 s_1 - 1\} \times \dots \times \{0, \dots, w_d s_d - 1\}$  for  $w \in \{1, 2, 3, \dots\}^d$ . For a standardized twice differentiable  $\sigma$ , there exist constants  $C_1, C_2 > 0$ , such that the following holds: for  $x, y \in \mathbb{S}_{n_0}^{I_0}$ , and any positions  $p, p' \in I_L$ , we have:*

**Freeze:** *When  $r_{\sigma,\beta} < 1$ , taking  $v = \min(v_s(p - p'), L - 1)$ , taking  $v = L - 1$  if  $p = p'$  and  $r = r_{\sigma,\beta}$ , we have*

$$\frac{1 - r^{v+1}}{1 - r^L} - C_1(v + 1)r^v \leq \vartheta_{p,p'}^{(L)}(x, y) \leq \frac{1 - r^{v+1}}{1 - r^L}.$$

**Chaos:** *When  $r_{\sigma,\beta} > 1$ , if either  $v_s(p - p') < L$  or if there exists a  $c < 1$  such that for all positions  $q \in I_0$  which are ancestor of  $p$ ,  $\left| x_q^T y_{q + \frac{p' - p}{s^L}} \right| < c$ , then there exists  $h < 1$  such that*

$$\left| \vartheta_{p,p'}^{(L)}(x, y) \right| \leq C_2 h^L.$$

This theorem suggests that in the freeze regime, the correlations between differing positions  $p$  and  $p'$  increase with  $v_s(p - p')$ , which is a strong feature of checkerboard patterns [20]. These artifacts typically appear in images generated by DC-NNs. The form of the NTK also suggests a strong affinity to these checkerboard patterns: they should dominate the NTK spectral decomposition. This is shown in Figure 2 where the eigenvectors of the NTK Gram matrix for a DC-NN are computed.

In the chaotic regime, the normalized NTK converges to a ‘scaled translation invariant’ Kronecker delta. For two output positions  $p$  and  $p' = p + ks^L$  we associate the two regions  $\omega$  and  $\omega' = \omega + k$  of the input space which are connected to  $p$  and  $p'$ . Then  $\vartheta_{p,p+ks^L}^{(L)}(x, y)$  is one if the patch  $y_{\omega'}$  is a  $k$  translation of  $x_\omega$  and approximately zero otherwise.

## 5 Batch Normalization, Hyperparameters and Nonlinearity Modifications

### 5.1 Batch Normalization

In Section 4, we have seen that in the frozen scenario, the NTK is dominated by the constant mode: more precisely, the constant functions correspond to the leading eigenvalue of the NTK. In this subsection, we explain how (a type of) Batch Normalization (BN) allows one to ‘kill’ the constant mode in the NTK. We consider the *post-nonlinearity* BN (PN-BN), which adds a normalizing layer to the activations (after the nonlinearity), defined by

$$\hat{\alpha}_k^{(\ell)}(x) = \frac{\alpha_k^{(\ell)}(x) - m_k(\theta)}{\sqrt{v_k(\theta) + \epsilon}},$$

for  $m_k(\theta) = \frac{1}{N} \sum_{i=1}^N \alpha_k^{(\ell)}(x_i)$ ,  $v_k(\theta) = \frac{1}{N} \sum \left( \alpha_k^{(\ell)}(x_i) - m_k(\theta) \right)^2$  and  $\epsilon > 0$ .

While incorporating the BN would modify the overparametrized regime of the NTK analysis, the following suggests that the PN-BN plays a role which can be understood in terms of the NTK. In particular, it allows to control the importance of the constant mode:

**Lemma 1.** *Consider FC-NN with  $L$  layers, with a PN-BN after the last nonlinearity, for any  $k, k' \in \{1, \dots, n_L\}$  and any parameter  $\theta_p$ , we have  $\sum_{i=1}^N \Theta_\theta^{(L)}(\cdot, x_i) = \beta^2 \text{Id}_{n_L}$ .*

When training the FC-NN with PN-BN to fit labels  $y_1, \dots, y_N \in \mathbb{R}^{n_L}$  with a small value  $\beta$ , it is important to center the labels, since the convergence is slow along the constant mode. On the other hand, a small value of  $\beta$  allows one to consider a higher learning rate, thus accelerating the convergence along the non-constant modes, including for large values of  $L$ .

## 5.2 Nonlinearity Normalization, Hyperparameter Tuning and Chaos-Freeze Transition

In Section 4, we showed the existence of the frozen and chaotic phases for FC-NNs and DC-NNs, which depends on the characteristic number  $r_{\sigma, \beta}$ . In this section, we show that by centering, standardizing the nonlinearity  $\sigma$  and by tuning  $\beta$ , one can reach both phases. Let us first observe that if we standardize  $\sigma$ , since as  $\beta \rightarrow 1$  we have  $r_{\sigma, \beta} \rightarrow 0$ , it is always possible to lie in the ordered regime. On the other hand, if we take a Lipschitz nonlinearity, by centering and standardizing  $\sigma$ , we can take  $\beta$  sufficiently small so that  $r_{\sigma, \beta} > 1$ , as guaranteed by the following (variant of Poincaré’s) lemma:

**Proposition 1.** *If  $\mathbb{E}_{x \sim \mathcal{N}(0,1)} [\sigma(x)] = 0$  and  $\mathbb{E}_{x \sim \mathcal{N}(0,1)} [\sigma^2(x)] = 1$ , we have  $\mathbb{E}_{x \sim \mathcal{N}(0,1)} [\dot{\sigma}^2(x)] > 1$ , in particular if*

$$\beta < \sqrt{1 - (\mathbb{E}_{x \sim \mathcal{N}(0,1)} [\dot{\sigma}^2(x)])^{-1}},$$

we have  $r_{\sigma, \beta} > 1$ .

**Remark 2.** *Centering and standardizing (i.e. normalizing) the nonlinearity  $\sigma$  is similar to Layer Normalization (LN) for FC-NNs, where for each input  $x \in \mathbb{R}^{n_0}$ , and each  $\ell = 1, \dots, L-1$ , we normalize the (post-nonlinearity) activation vectors  $\alpha^{(\ell)}(x)$  to center and normalize their entries:*

$$\check{\alpha}^{(\ell)}(x) = \sqrt{n_\ell} \frac{\alpha^{(\ell)}(x) - \frac{1}{n_\ell} \sum_{i=1}^{n_\ell} \alpha_i^{(\ell)}(x)}{\|\alpha^{(\ell)}(x) - \frac{1}{n_\ell} \sum_{i=1}^{n_\ell} \alpha_i^{(\ell)}(x)\|}.$$

*In the infinite-width limit, normalizing  $\sigma$  is equivalent to LN if the input datapoints have a norm  $\sqrt{n_0}$ . For more details, see Appendix C.*

## 6 New NTK Parametrization: Boundary Effects and Learning Rates

In DC-NNs, the neurons which lie at position  $p$  on the border of the patches  $I_\ell$  behave differently than neurons in the center. Typically, these neurons have less parent neurons in the precedent layer and as result have a lower variance at initialization. Both kernels  $\Sigma_{pp}^{(\ell)}$  and  $\Theta_{pp}^{(\ell)}$  have lower intensity for  $p \in I_\ell$  on the border (see Appendix G for an example when  $I_\ell = \mathbb{N}$ , i.e. when there is one border pixel), which leads to border artifacts as seen in Figure 2.

A natural solution is to adapt the factors in the definition of the DC filters. Instead of dividing by (the squared root of)  $|\omega|_{s_1, \dots, s_d}$  which is the maximal number of parents (only attained in center neurons) we divide by the actual number of parents  $|\pi(p)| = |\{q \in I_\ell : sq \in p + \omega\}|$ :

$$y_q = \frac{\sqrt{1 - \beta^2}}{\sqrt{n_\ell |\pi(p)|}} W^{(\ell)}(x_{p+\omega}) + \beta b^{(\ell)},$$

In the Appendix E, in order to be self-contained and since we consider up-sampling, we show again that the NTK converges as the width of the layers grow to infinity sequentially. By doing so, we get formulae for the limiting NTK which allow us to prove that, with the parent-based parametrization, the border artifacts disappear for both  $\Sigma^{(\ell)}$  and  $\Theta_\infty^{(\ell)}$ :

**Proposition 2.** *For the parent-based parametrization of DC-NNs, if the non-linearity is standardized,  $(\Sigma^{(L)})_{pp}(x)$  and  $(\Theta_\infty^{(L)})_{pp}(x)$  do not depend neither on  $p \in I_L$  nor on  $x \in \mathbb{S}_{n_0}^{I_0}$ .*

### 6.1 Layer-dependent learning rate

The NTK is the sum  $\Theta^{(L)} = \sum_\ell \Theta^{(L; W^{(\ell)})} + \Theta^{(L; b^{(\ell)})}$  over the contributions of the weights  $\Theta_{pq}^{(L; W^{(\ell)})}(x, y) = \sum_{ij} \partial_{W_{ij}^{(\ell)}} f_{\theta, p}(x) \partial_{W_{ij}^{(\ell)}} f_{\theta, q}(y)$  and biases  $\Theta_{pq}^{(L; b^{(\ell)})}(x, y) =$

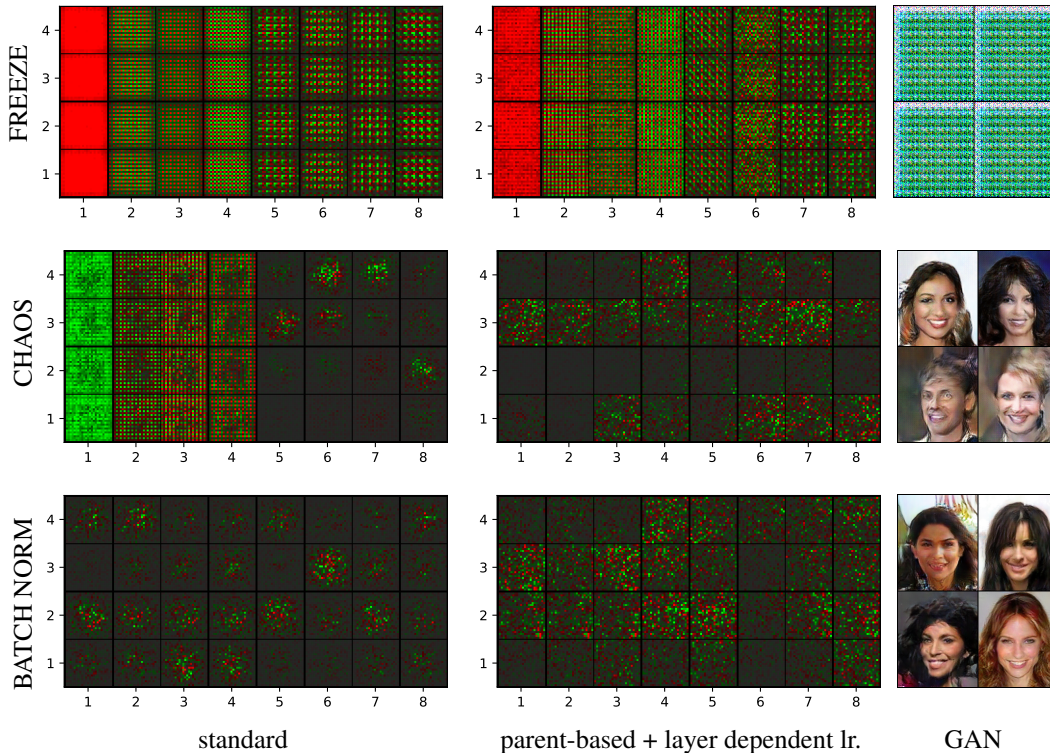


Figure 2: The first 8 eigenvectors of the NTK Gram matrix of a DC-NN ( $L=3$ ) on 4 inputs (left) with the parametrization of Section 2.2 and (middle) with the proposed modifications of Section 6 (right) results of a GAN on CelebA. Each line correspond to a choice of non-linearity/normalization for the generator: (top) ReLU, (middle) normalized ReLU and (bottom) ReLU with Batch Normalization.

$\sum_j \partial_{b_j^{(\ell)}} f_{\theta,p}(x) \partial_{b_j^{(\ell)}} f_{\theta,q}(y)$ . At the  $\ell$ -th layer, the weights and biases can only contribute to checkerboard patterns of degree  $v = L - \ell$  and  $v = L - \ell - 1$ , i.e. patterns with periods  $s^{L-\ell}$  and  $s^{L-\ell-1}$  respectively, in the following sense:

**Proposition 3.** *In a DC-NN with stride  $s \in \{2, 3, \dots\}^d$ , we have  $\Theta_{\infty, pp'}^{(L:W^{(\ell)})}(x, y) = 0$  if  $s^{L-\ell} \nmid p' - p$  and  $\Theta_{\infty, pp'}^{(L:b^{(\ell)})}(x, y) = 0$  if  $s^{L-\ell-1} \nmid p' - p$ .*

This suggests that the supports of  $\Theta_{\infty}^{(L:W^{(\ell)})}$  and  $\Theta_{\infty}^{(L:b^{(\ell)})}$  increase exponentially with  $\ell$ , giving more importance to the last layers during training. This could explain why the checkerboard patterns of lower degree dominate in Figure 2. In the classical parametrization, the balance is restored by letting the number of channels  $n_\ell$  decrease with depth [23]. In the NTK parametrization, the limiting NTK is not affected by the ratios  $n_\ell/n_k$ . To achieve the same effect, we divide the learning rate of the weights and bias of the  $\ell$ -th layer by  $S^{\ell/2}$  and  $S^{(\ell+1)/2}$  respectively, where  $S = \prod_i s_i$  is the product of the strides.

Together with the ‘parent-based’ parametrization and the normalization of the non-linearity (in order to lie in the chaotic regime) this rescaling of the learning rate removes both border and checkerboard artifacts in Figure 2.

## 7 Generative Adversarial Networks

A common problem in the training of GANs is the collapse of the generator to a constant. This problem is greatly reduced by avoiding the ‘freeze’ regime in which the constant mode dominates and by using the new NTK parametrization with adaptive learning rates. Figure 2 shows the results obtained with three GANs which differ only in the choice of non-linearity and/or the presence of



Batch Normalization in the generator. In all cases, the discriminator is a convolutional network with the normalized ReLU as non-linearity. With the ReLU, the generator collapses and generates a single image with checkerboard patterns. With the normalized ReLU or with Batch Normalization, the generator is able to learn a variety of images. This motivates the use of normalization techniques in GANs to avoid the collapse of the generator.

## 8 Conclusion

This article shows how the NTK can be used theoretically to understand the effect of architecture choices (such as decreasing the number of channels or batch normalization) on the training of DNNs. We have shown that DNNs in a “freeze” regime, have a strong affinity to constant modes and checkerboard artifacts: this slows down training and can contribute to a mode collapse of the DC-NN generator of GANs. We introduce simple modifications to solve these problems: the effectiveness of normalizing the non-linearity, a parent-based parametrization and a layer-dependent learning rates is shown both theoretically and numerically.

## References

- [1] Allen-Zhu, Zeyuan, Li, Yuanzhi, & Song, Zhao. 2018. A Convergence Theory for Deep Learning via Over-Parameterization. *CoRR*, **abs/1811.03962**.
- [2] Arora, Sanjeev, Du, Simon S, Hu, Wei, Li, Zhiyuan, Salakhutdinov, Ruslan, & Wang, Ruosong. 2019. On Exact Computation with an Infinitely Wide Neural Net. *arXiv preprint arXiv:1904.11955*.
- [3] Arpit, Devansh, Zhou, Yingbo, Kota, Bhargava, & Govindaraju, Venu. 2016. Normalization Propagation: A Parametric Technique for Removing Internal Covariate Shift in Deep Networks. *Pages 1168–1176 of: Balcan, Maria Florina, & Weinberger, Kilian Q. (eds), Proceedings of The 33rd International Conference on Machine Learning*. Proceedings of Machine Learning Research, vol. 48. New York, New York, USA: PMLR.
- [4] Brock, Andrew, Donahue, Jeff, & Simonyan, Karen. 2018. Large scale gan training for high fidelity natural image synthesis. *arXiv preprint arXiv:1809.11096*.
- [5] Cho, Youngmin, & Saul, Lawrence K. 2009. Kernel Methods for Deep Learning. *Pages 342–350 of: Advances in Neural Information Processing Systems 22*. Curran Associates, Inc.
- [6] Daniely, Amit, Frostig, Roy, & Singer, Yoram. 2016. Toward Deeper Understanding of Neural Networks: The Power of Initialization and a Dual View on Expressivity. *Pages 2253–2261 of: Lee, D. D., Sugiyama, M., Luxburg, U. V., Guyon, I., & Garnett, R. (eds), Advances in Neural Information Processing Systems 29*. Curran Associates, Inc.
- [7] Du, Simon S., Zhai, Xiyu, Póczos, Barnabás, & Singh, Aarti. 2019. Gradient Descent Provably Optimizes Over-parameterized Neural Networks.
- [8] Dumoulin, Vincent, & Visin, Francesco. 2016. A guide to convolution arithmetic for deep learning. *arXiv preprint arXiv:1603.07285*.
- [9] Glorot, Xavier, & Bengio, Yoshua. 2010. Understanding the difficulty of training deep feedforward neural networks. *Pages 249–256 of: Proceedings of the Thirteenth International Conference on Artificial Intelligence and Statistics*. Proceedings of Machine Learning Research, vol. 9. Chia Laguna Resort, Sardinia, Italy: PMLR.
- [10] Goodfellow, Ian J., Pouget-Abadie, Jean, Mirza, Mehdi, Xu, Bing, Warde-Farley, David, Ozair, Sherjil, Courville, Aaron, & Bengio, Yoshua. 2014. Generative Adversarial Networks. *NIPS’14 Proceedings of the 27th International Conference on Neural Information Processing Systems - Volume 2*, jun, 2672–2680.
- [11] Ioffe, Sergey, & Szegedy, Christian. 2015. Batch Normalization: Accelerating Deep Network Training by Reducing Internal Covariate Shift. *CoRR*, **abs/1502.03167**.

- [12] Jacot, Arthur, Gabriel, Franck, & Hongler, Clément. 2018. Neural Tangent Kernel: Convergence and Generalization in Neural Networks. *Pages 8580–8589 of: Advances in Neural Information Processing Systems 31*. Curran Associates, Inc.
- [13] Karakida, Ryo, Akaho, Shotaro, & Amari, Shun-Ichi. 2018. Universal Statistics of Fisher Information in Deep Neural Networks: Mean Field Approach. *jun*.
- [14] Karras, Tero, Laine, Samuli, & Aila, Timo. 2018. A style-based generator architecture for generative adversarial networks. *arXiv preprint arXiv:1812.04948*.
- [15] Klambauer, Günter, Unterthiner, Thomas, Mayr, Andreas, & Hochreiter, Sepp. 2017. Self-Normalizing Neural Networks. *Pages 971–980 of: Guyon, I., Luxburg, U. V., Bengio, S., Wallach, H., Fergus, R., Vishwanathan, S., & Garnett, R. (eds), Advances in Neural Information Processing Systems 30*. Curran Associates, Inc.
- [16] LeCun, Yann A, Bottou, Léon, Orr, Genevieve B, & Müller, Klaus-Robert. 2012. Efficient backprop. *Pages 9–48 of: Neural networks: Tricks of the trade*. Springer.
- [17] Lee, Jae Hoon, Bahri, Yasaman, Novak, Roman, Schoenholz, Samuel S., Pennington, Jeffrey, & Sohl-Dickstein, Jascha. 2018. Deep Neural Networks as Gaussian Processes. *ICLR*.
- [18] Lei Ba, J., Kiros, J. R., & Hinton, G. E. 2016. Layer Normalization. *arXiv e-prints*, July.
- [19] Neal, Radford M. 1996. *Bayesian Learning for Neural Networks*. Secaucus, NJ, USA: Springer-Verlag New York, Inc.
- [20] Odena, Augustus, Dumoulin, Vincent, & Olah, Chris. 2016. Deconvolution and checkerboard artifacts. *Distill*, **1**(10), e3.
- [21] Park, Daniel S, Smith, Samuel L, Sohl-dickstein, Jascha, & Le, Quoc V. 2018. Optimal SGD Hyperparameters for Fully Connected Networks.
- [22] Poole, Ben, Lahiri, Subhaneil, Raghu, Maithra, Sohl-Dickstein, Jascha, & Ganguli, Surya. 2016. Exponential expressivity in deep neural networks through transient chaos. *Pages 3360–3368 of: Lee, D. D., Sugiyama, M., Luxburg, U. V., Guyon, I., & Garnett, R. (eds), Advances in Neural Information Processing Systems 29*. Curran Associates, Inc.
- [23] Radford, Alec, Metz, Luke, & Chintala, Soumith. 2015. Unsupervised representation learning with deep convolutional generative adversarial networks. *arXiv preprint arXiv:1511.06434*.
- [24] Salimans, Tim, & Kingma, Durk P. 2016. Weight Normalization: A Simple Reparameterization to Accelerate Training of Deep Neural Networks. *Pages 901–909 of: Lee, D. D., Sugiyama, M., Luxburg, U. V., Guyon, I., & Garnett, R. (eds), Advances in Neural Information Processing Systems 29*. Curran Associates, Inc.
- [25] Santurkar, Shibani, Tsipras, Dimitris, Ilyas, Andrew, & Madry, Aleksander. 2018. How Does Batch Normalization Help Optimization? *Pages 2483–2493 of: Bengio, S., Wallach, H., Larochelle, H., Grauman, K., Cesa-Bianchi, N., & Garnett, R. (eds), Advances in Neural Information Processing Systems 31*. Curran Associates, Inc.
- [26] Xiang, Sitao, & Li, Hao. 2017. On the effects of batch and weight normalization in generative adversarial networks. *arXiv preprint arXiv:1704.03971*.
- [27] Yang, Greg. 2019. Scaling Limits of Wide Neural Networks with Weight Sharing: Gaussian Process Behavior, Gradient Independence, and Neural Tangent Kernel Derivation. *arXiv e-prints*, Feb, arXiv:1902.04760.
- [28] Yang, Greg, & Schoenholz, Samuel. 2017. Mean Field Residual Networks: On the Edge of Chaos. *Pages 7103–7114 of: Guyon, I., Luxburg, U. V., Bengio, S., Wallach, H., Fergus, R., Vishwanathan, S., & Garnett, R. (eds), Advances in Neural Information Processing Systems 30*. Curran Associates, Inc.
- [29] Yang, Greg, Pennington, Jeffrey, Rao, Vinay, Sohl-Dickstein, Jascha, & Schoenholz, Samuel S. 2019. A Mean Field Theory of Batch Normalization. *CoRR*, **abs/1902.08129**.
- [30] Zhang, Han, Goodfellow, Ian, Metaxas, Dimitris, & Odena, Augustus. 2018. Self-attention generative adversarial networks. *arXiv preprint arXiv:1805.08318*.

## A Choice of Parametrization

The NTK parametrization differs slightly from the one usually used, yet it ensures that the training is consistent as the size of the layers grows. In the standard parametrization, the activations are defined by

$$\begin{aligned}\alpha^{(0)}(x; \theta) &= x \\ \tilde{\alpha}^{(\ell+1)}(x; \theta) &= W^{(\ell)} \alpha^{(\ell)}(x; \theta) + b^{(\ell)} \\ \alpha^{(\ell+1)}(x; \theta) &= \sigma \left( \tilde{\alpha}^{(\ell+1)}(x; \theta) \right),\end{aligned}$$

and we denote by  $g_\theta$  the output function of the ANN. Note the absence of  $1/\sqrt{n_\ell}$  in comparison to the NTK parametrization. The parameters are initialized using the LeCun/He initialization [16]: the parameters  $W^{(\ell)}$  have standard deviation  $1/\sqrt{n_\ell}$  (or  $\sqrt{2}/\sqrt{n_\ell}$  for the ReLU but this does not change the general analysis). Using this initialization, the activations stay stochastically bounded as the widths of the ANN get large. In the forward pass, there is almost no difference between the two parametrizations and for each choice of parameters  $\theta$ , we can scale down the connection weights by  $\sqrt{1-\beta^2}/\sqrt{n_\ell}$  and the bias weights by  $\beta$  to obtain a new set of parameters  $\hat{\theta}$  such that

$$f_\theta = g_{\hat{\theta}}.$$

The two parametrizations will exhibit a difference during backpropagation since:

$$\partial_{W_{ij}^{(\ell)}} g_{\hat{\theta}}(x) = \frac{\sqrt{n_\ell}}{\sqrt{1-\beta^2}} \partial_{W_{ij}^{(\ell)}} f_\theta(x), \quad \partial_{b_j^{(\ell)}} g_{\hat{\theta}}(x) = \frac{1}{\beta} \partial_{b_j^{(\ell)}} f_\theta(x).$$

The NTK is a sum of products of these derivatives over all parameters:

$$\Theta^{(L)} = \Theta^{(L:W^{(0)})} + \Theta^{(L:b^{(0)})} + \Theta^{(L:W^{(1)})} + \Theta^{(L:b^{(1)})} + \dots + \Theta^{(L:W^{(L-1)})} + \Theta^{(L:b^{(L-1)})}.$$

With our parametrization, all summands converge to a finite limit, while with the Le Cun or He parameterization we obtain

$$\hat{\Theta}^{(L)} = \frac{n_0}{1-\beta^2} \Theta^{(L:W^{(0)})} + \frac{1}{\beta^2} \Theta^{(L:b^{(0)})} + \dots + \frac{n_{L-1}}{1-\beta^2} \Theta^{(L:W^{(L-1)})} + \frac{1}{\beta^2} \Theta^{(L:b^{(L-1)})},$$

where some summands, namely the  $\left(\frac{n_i}{1-\beta^2} \Theta^{(L:W^{(i)})}\right)_i$ , explode in the infinite width limit. One must therefore take a learning rate of order  $1/\max(n_1, \dots, n_{L-1})$  [13, 21] to obtain a meaningful training dynamics, but in this case the contributions to the NTK of the first layers connections  $W^{(0)}$  and the bias of all layers  $b^{(\ell)}$  vanish, which implies that training these parameters has less and less effect on the function as the width of the network grows. As a result, the dynamics of the output function during training can still be described by a modified kernel gradient descent: the modified learning rate compensates for the absence of normalization in the usual parametrization.

The NTK parametrization is hence more natural for large networks, as it solves both the problem of having a meaningful forward and backward passes, and to avoid tuning the learning rate, which is the problem that sparked multiple alternative initialization strategies in deep learning [9]. Note that in the standard parametrization, the importance of the bias parameters shrinks as the width gets large; this can be implemented in the NTK parametrization by taking a small value for the parameter  $\beta$ .

## B FC-NN Freeze and Chaos

In this section, we prove Theorem 2, showing the existence of two regimes, ‘freeze’ and ‘chaos’, in FC-NNs. First, we improve some results of [6], and study the rate of convergence of the activation kernels as the depth grows to infinity. In a second step, this allows us to characterise the behavior of the NTK for large depth.

Let us consider a standardized differentiable non-linearity  $\sigma$ , i.e. satisfying  $\mathbb{E}_{x \sim \mathcal{N}(0,1)} [\sigma^2(x)] = 1$ . Recall that the activation kernels are defined recursively by  $\Sigma^{(1)}(x, y) = \frac{1-\beta^2}{n_0} x^T y + \beta^2$  and



Figure 3: Result of two GANs on CelebA. (Left) with Nonlinearity Normalization and (Right) with Batch Normalization. In both cases the discriminator uses a Normalized ReLU.

$\Sigma^{(\ell+1)}(x, y) = (1 - \beta^2)\mathbb{L}_{\Sigma^{(\ell)}}^{\sigma}(x, y) + \beta^2$ . By induction, for any  $x, y \in \mathbb{S}_{n_0}$ ,  $\Sigma^{(\ell+1)}(x, y)$  is uniquely determined by  $\rho_{x,y} = \frac{1}{n_0}x^T y$ . Defining the two functions  $R_{\sigma}, B_{\beta} : [-1, 1] \rightarrow [-1, 1]$  by:

$$R_{\sigma}(\rho) = \mathbb{E}_{v \sim \mathcal{N}\left(0, \begin{pmatrix} 1 & \rho \\ \rho & 1 \end{pmatrix}\right)} [\sigma(v_0)\sigma(v_1)],$$

$$B_{\beta}(\rho) = \beta^2 + (1 - \beta^2)\rho,$$

one can formulate the activation kernels as an alternate composition of  $B_{\beta}$  and  $R_{\sigma}$ :

$$\Sigma^{(\ell)}(x, y) = (B_{\beta} \circ R_{\sigma})^{\circ \ell - 1} \circ B_{\beta}(\rho_{x,y}).$$

In particular, this shows that for any  $x, y \in \mathbb{S}_{n_0}$ ,  $\Sigma^{(\ell)}(x, y) \leq 1$ . Since the activation kernels are obtained by iterating the same function, we first study the fixed points of the composition  $B_{\beta} \circ R_{\sigma} : [-1, 1] \rightarrow [-1, 1]$ . When  $\sigma$  is a standardized non-linearity, the function  $R_{\sigma}$ , named the dual of  $\sigma$ , satisfies the following key properties proven in [6]:

1.  $R_{\sigma}(1) = 1$ ,
2. For any  $\rho \in (-1, 0)$ ,  $R_{\sigma}(\rho) > \rho$ ,
3.  $R_{\sigma}$  is convex in  $[0, 1)$ ,
4.  $R'_{\sigma}(1) = \mathbb{E}[\dot{\sigma}(x)^2]$ , where  $R'_{\sigma}$  denotes the derivative of  $R_{\sigma}$ ,
5.  $R'_{\sigma} = R_{\dot{\sigma}}$ .

By definition  $B_{\beta}(1) = 1$ , thus 1 is a trivial fixed point:  $B_{\beta} \circ R_{\sigma}(1) = 1$ . This shows that for any  $x \in \mathbb{S}_{n_0}$  and any  $\ell \geq 1$ :

$$\Sigma^{(\ell)}(x, x) = 1.$$

It appears that  $-1$  is also a fixed point of  $B_{\beta} \circ R_{\sigma}$  if and only if the non-linearity  $\sigma$  is antisymmetric and  $\beta = 0$ . From now on, we will focus on the region  $(-1, 1)$ . From the property 2. of  $R_{\sigma}$  and since  $B_{\beta}$  is non decreasing, any non trivial fixed point must lie in  $[0, 1)$ . Since  $B_{\beta} \circ R_{\sigma}(0) > 0$ ,  $B_{\beta} \circ R_{\sigma}(1) = 1$  and  $R_{\sigma}$  is convex in  $[0, 1)$ , there exists a non trivial fixed point of  $B_{\beta} \circ R_{\sigma}$  if  $(B_{\beta} \circ R_{\sigma})'(1) > 1$  whereas if  $(B_{\beta} \circ R_{\sigma})'(1) < 1$  there is no fixed point in  $(-1, 1)$ . This leads to two regimes shown in [6], depending on the value of  $r_{\sigma,\beta} = (1 - \beta^2) \mathbb{E}_{x \sim \mathcal{N}(0,1)}[\dot{\sigma}^2(x)]$ :

1. “Freeze” when  $r_{\sigma,\beta} < 1$ :  $B_{\beta} \circ R_{\sigma}$  has a unique fixed point equal to 1 and the activation kernels become constant at an exponential rate,

2. “Chaos” when  $r_{\sigma,\beta} > 1$ :  $B_\beta \circ R_\sigma$  has another fixed point  $0 \leq a < 1$  and the activation kernels converge to a kernel equal to 1 if  $x = y$  and to  $a$  if  $x \neq y$  and, if the nonlinearity is antisymmetric and  $\beta = 0$ , it converges to  $-1$  if and only if  $x = -y$ .

To establish the existence of the two regimes for the NTK, we need the following bounds on the rate of convergence of  $\Sigma^{(\ell)}(x, y)$  in the “freeze” region and on its values in the “chaos” region:

**Lemma 2.** *If  $\sigma$  is a standardized differentiable non-linearity,*

*If  $r_{\sigma,\beta} < 1$ , then for any  $x, y \in \mathbb{S}_{n_0}$ ,*

$$1 \geq \Sigma^{(\ell)}(x, y) \geq 1 - 2r_{\sigma,\beta}^{\ell-1}(1 - \beta^2).$$

*If  $r_{\sigma,\beta} > 1$ , then there exists a fixed point  $a \in [0, 1)$  of  $B_\beta \circ R_\sigma$  such that for any  $x, y \in \mathbb{S}_{n_0}$ ,*

$$\left| \Sigma^{(\ell)}(x, y) \right| \leq \max \left\{ \left| \beta^2 + \frac{1 - \beta^2}{n_0} x^T y \right|, a \right\}.$$

*Proof.* Let us denote  $r = r_{\sigma,\beta}$ . Let us suppose that  $r_{\sigma,\beta} < 1$ . By [6], we know that  $R'_\sigma = R_{\dot{\sigma}}$  and  $R_{\dot{\sigma}}(\rho) \in [-\mathbb{E}[\dot{\sigma}(z)^2], \mathbb{E}[\dot{\sigma}(z)^2]]$  where  $z \sim \mathcal{N}(0, 1)$ . From now on, we will omit to specify the distribution assumption on  $z$ . The previous equalities and inequalities imply that  $R_\sigma(\rho) \geq 1 - \mathbb{E}[\dot{\sigma}(v)^2](1 - \rho)$ , thus we obtain:

$$\begin{aligned} B_\beta \circ R_\sigma(\rho) &\geq \beta^2 + (1 - \beta^2)(1 - \mathbb{E}[\dot{\sigma}(z)^2](1 - \rho)) \\ &= 1 - (1 - \beta^2)\mathbb{E}[\dot{\sigma}(z)^2](1 - \rho) \\ &= 1 - r(1 - \rho). \end{aligned}$$

By definition, we then have  $\Sigma^{(\ell)}(x, y) = (B_\beta \circ R_\sigma)^{\circ \ell-1} \circ B_\beta \left( \frac{1}{n_0} x^T y \right) \geq 1 - 2(1 - \beta^2)r^{\ell-1}$ .

Using the bound  $\Sigma^{(\ell)}(x, y) \leq 1$ , this proves the first assertion.

When  $r > 1$ , there exists a fixed point  $a$  of  $B_\beta \circ R_\sigma$  in  $[0, 1)$ . By convexity argument, for any  $\rho$  in  $[a, 1)$ ,  $a \leq B_\beta \circ R_\sigma(\rho) \leq \rho$  and because  $R_\sigma(\rho)$  is increasing in  $[0, 1)$ , for all  $\rho \in [0, a]$ ,  $0 \leq B_\beta \circ R_\sigma(\rho) \leq a$ .

For negative  $\rho$ , it follows from the fact that  $|B_\beta \circ R_\sigma(\rho)| \leq B_\beta \circ R_\sigma(|\rho|)$ : because  $R_\sigma(\rho) = \sum_{i=0}^{\infty} b_i \rho^i$  for positive  $b_i$ s [6], and the composition  $B_\beta \circ R_\sigma(\rho) = \sum_{i=0}^{\infty} c_i \rho^i$  for  $c_0 = b_0(1 - \beta^2) + \beta^2 \geq 0$  and  $c_i = b_i(1 - \beta^2) \geq 0$  when  $i > 0$ , we have

$$|B_\beta \circ R_\sigma(\rho)| = \left| \sum_{i=0}^{\infty} c_i \rho^i \right| \leq \sum_{i=0}^{\infty} c_i |\rho|^i = B_\beta \circ R_\sigma(|\rho|).$$

This leads to the inequality in the chaos region.  $\square$

Before studying the normalized NTK, let us remark that the NTK on the diagonal (with  $x = y$  in  $\mathbb{S}_{n_0}$ ) is equal to:

$$\begin{aligned} \Theta_\infty^{(L)}(x, x) &= \sum_{\ell=1}^L \Sigma^{(\ell)}(x, x) \prod_{k=\ell+1}^L \dot{\Sigma}^{(k)}(x, x) \\ &= \sum_{\ell=1}^L ((1 - \beta^2)\mathbb{E}[\dot{\sigma}(x)^2])^{L-\ell} \\ &= \frac{1 - r_{\sigma,\beta}^L}{1 - r_{\sigma,\beta}}. \end{aligned}$$

This shows that in the “freeze” regime,  $\Theta_\infty^{(L)}(x, x) \xrightarrow{L \rightarrow \infty} 1/1 - r_{\sigma,\beta}$  and in the “chaos” regime  $\Theta_\infty^{(L)}(x, x)$  grows exponentially. At the transition  $r_{\sigma,\beta} = 1$  and thus  $\Theta_\infty^{(L)}(x, x) = L$ . Besides, if  $x, y \in \mathbb{S}_{n_0}$ , using the Cauchy-Schwarz inequality, for any  $\ell$ ,  $|\Sigma^{(\ell)}(x, y)| \leq |\Sigma^{(\ell)}(x, x)|$  and  $|\dot{\Sigma}^{(\ell+1)}(x, y)| \leq |\dot{\Sigma}^{(\ell+1)}(x, x)|$ . This implies the following inequality:  $\Theta_\infty^{(L)}(x, y) \leq \Theta_\infty^{(L)}(x, x)$ .

We now study the normalized NTK  $\vartheta_L(x, y) = \frac{\Theta_\infty^{(L)}(x, y)}{\Theta_\infty^{(L)}(x, x)} \leq 1$ .

**Theorem 2.** Suppose that  $\sigma$  is twice differentiable and standardized.

If  $r_{\sigma,\beta} < 1$ , we are in the frozen regime: there exists  $C_1$  such that for  $x, y \in \mathbb{S}_{n_0}$ ,

$$1 - C_1 L r_{\sigma,\beta}^L \leq \vartheta^{(L)}(x, y) \leq 1.$$

If  $r_{\sigma,\beta} > 1$ , we are in the chaotic regime: for  $x \neq y$  in  $\mathbb{S}_{n_0}$ , there exist  $s < 1$  and  $C_2$ , such that

$$\left| \vartheta^{(L)}(x, y) \right| \leq C_2 s^L.$$

*Proof.* Let us denote  $r = r_{\sigma,\beta}$ . First, let us suppose that  $r < 1$ . Recall that the NTK is defined as

$$\Theta_\infty^{(L)}(x, y) = \sum_{\ell=1}^L \Sigma^{(\ell)}(x, y) \dot{\Sigma}^{(\ell+1)}(x, y) \dots \dot{\Sigma}^{(L)}(x, y).$$

For all  $\ell$ ,  $\Sigma^{(\ell)}(x, y) \leq \Sigma^{(\ell)}(x, x) = 1$  and  $\dot{\Sigma}^{(\ell)}(x, y) \leq \dot{\Sigma}^{(\ell)}(x, x) = r$ . Writing  $\Sigma^{(\ell)}(x, y) = 1 - \epsilon^{(\ell)}$  and  $\Sigma^{(\ell)}(x, y) = 1 - \dot{\epsilon}^{(\ell)}$  for  $\epsilon^{(\ell)}, \dot{\epsilon}^{(\ell)} \geq 0$  we have

$$\begin{aligned} \Theta_\infty^{(L)}(x, y) &= \sum_{\ell=1}^L (1 - \epsilon^{(\ell)}) \prod_{k=\ell+1}^L r - \dot{\epsilon}^{(\ell)} \\ &\leq \sum_{\ell=1}^L r^{L-\ell} - r^{L-\ell} \epsilon^{(\ell)} - \sum_{k=\ell+1}^L r^{L-\ell-1} \dot{\epsilon}^{(k)} \end{aligned}$$

Using the bound of Lemma 2 and the fact that for any  $x, y \in \mathbb{S}_{n_0}$ ,  $\dot{\Sigma}^{(\ell)}(x, y) = (1 - \beta^2) R_{\dot{\sigma}}(\Sigma^{(\ell-1)}(x, y)) \geq r - \psi \epsilon^{(\ell-1)}$  for  $\psi = (1 - \beta^2) \mathbb{E}_{z \sim \mathcal{N}(0,1)} [\dot{\sigma}(z)]$ , we obtain  $\epsilon^{(\ell)} < 2(1 - \beta^2) r^{\ell-1}$  and  $\dot{\epsilon}^{(\ell)} \leq 2(1 - \beta^2) \psi r^{\ell-2}$ . As a result:

$$\begin{aligned} \Theta_\infty^{(L)}(x, y) &\geq \sum_{\ell=1}^L r^{L-\ell} - 2(1 - \beta^2) r^{L-\ell} r^{\ell-1} - \sum_{k=\ell+1}^L 2(1 - \beta^2) \psi r^{L-\ell-1} r^{k-2} \\ &= \Theta_\infty^{(L)}(x, x) - 2(1 - \beta^2) \sum_{\ell=1}^L r^{L-1} + \psi \sum_{k=\ell+1}^L r^{L-\ell+k-3} \\ &= \Theta_\infty^{(L)}(x, x) - 2(1 - \beta^2) \left[ L r^{L-1} + \psi \sum_{\ell=1}^L \sum_{k=0}^{L-\ell-1} r^{L+k-2} \right] \\ &= \Theta_\infty^{(L)}(x, x) - 2(1 - \beta^2) \left[ L r^{L-1} + \psi r^{L-2} \sum_{\ell=1}^L \frac{1 - r^{L-\ell}}{1 - r} \right] \\ &\geq \Theta_\infty^{(L)}(x, x) - 2(1 - \beta^2) \left[ r + \psi \frac{1}{1 - r} \right] L r^{L-2} \\ &\geq \Theta_\infty^{(L)}(x, x) - C L r^L. \end{aligned}$$

Now, let us suppose that  $r > 1$ . Recall that  $B_\beta \circ R_\sigma$  has a unique fixed point  $a$  on  $[0, 1]$ . For any  $x$  and  $y$  in  $\mathbb{S}_{n_0}$ , the kernels  $\Sigma^{(\ell)}(x, y)$  are bounded in norm by  $v = \max \left\{ \left| \beta^2 + \frac{1-\beta^2}{n_0} x^T y \right|, a \right\}$  from Lemma 2. For the kernels  $\dot{\Sigma}^{(\ell)}$  we have  $\left| \dot{\Sigma}^{(\ell)}(x, y) \right| = (1 - \beta^2) |R_{\dot{\sigma}}(\Sigma^{(\ell-1)}(x, y))| \leq (1 - \beta^2) R_{\dot{\sigma}}(|\Sigma^{(\ell-1)}(x, y)|) \leq (1 - \beta^2) R_{\dot{\sigma}}(v) =: w$  where the first inequality follows from the fact that  $R_{\dot{\sigma}}(\rho) = \sum_i b_i \rho^i$  for  $b_i \geq 0$  and the second follows from the monotonicity of  $R_{\dot{\sigma}}$  in  $[0, 1]$ . Applying these two bounds, we obtain:

$$\left| \Theta_\infty^{(L)}(x, y) \right| \leq \sum_{\ell=1}^L v \prod_{k=\ell+1}^L w = v \frac{1 - w^L}{1 - w}.$$

Since  $\Theta_\infty^{(L)}(x, y) = \frac{1-r^L}{1-r}$ , we have that  $|\vartheta_L(x, y)| \leq v \frac{1-w^L}{1-r^L}$ . If  $x \neq y$  then  $v < 1$  and since  $\sigma$  is non-linear,  $w = (1 - \beta^2) R_{\dot{\sigma}}(v) < (1 - \beta^2) R_{\dot{\sigma}}(1) = r$ . This implies that  $|\vartheta_L(x, y)|$  converges to zero at an exponential rate.  $\square$

## B.1 ReLU FC-NN

For the standardized ReLU non-linearity,  $\sigma(x) = \sqrt{2} \max(x, 0)$ , the dual activation is computed in [6]:

$$R_\sigma(\rho) = \frac{\sqrt{1-\rho^2} + (\pi - \cos^{-1}(\rho))\rho}{\pi},$$

and the dual activation of its derivative is given by:

$$R_{\dot{\sigma}}(\rho) = \frac{\pi - \cos^{-1}(\rho)}{\pi}.$$

The characteristic value  $r_{\sigma,\beta}$  of the standardized ReLU is equal to  $1 - \beta^2$ : the ReLU non-linearity therefore lies in the “freeze” regime as soon as  $\beta > 0$ . More explicitly, Lemma 2 still holds of the standardized ReLU and, using the value of  $r_{\sigma,\beta}$ , the following inequalities hold for any  $x, y \in \mathbb{S}_{n_0}$ :

$$1 \geq \Sigma^{(\ell)}(x, y) \geq 1 - 2r_{\sigma,\beta}^\ell.$$

Using these bounds, we can now prove Theorem 3.

**Theorem 3.** *With the same notation as in Theorem 2, taking  $\sigma$  to be the standardized ReLU and  $\beta > 0$ , we are in the weakly frozen regime: there exists a constant  $C$  such that  $1 - CLr_{\sigma,\beta}^{L/2} \leq \vartheta^{(L)}(x, y) \leq 1$ .*

*Proof.* Let us denote  $r = r_{\sigma,\beta}$ . The first inequality  $\vartheta_L(x, y) \leq 1$  follows the same proof as in the differentiable case.

For the lower bound, using the fact that  $(1 - \beta)r = 1$ , we have  $\epsilon^{(\ell)} = 1 - \Sigma^{(\ell)}(x, y) \leq 2r^\ell$  and using the explicit value of  $R_{\dot{\sigma}}(\rho)$ , we get that  $R_{\dot{\sigma}}(\rho) \geq 1 - \sqrt{1 - \rho}$  which implies that  $\dot{\epsilon}^{(\ell)} = r - \dot{\Sigma}^{(\ell)}(x, y) \leq r\sqrt{2}r^{\frac{\ell-1}{2}}$ :

$$\begin{aligned} \Theta_\infty^{(L)}(x, y) &= \sum_{\ell=1}^L \left(1 - \epsilon^{(\ell)}\right) \prod_{k=\ell+1}^L r - \dot{\epsilon}^{(k)} \\ &\geq \sum_{\ell=1}^L r^{L-\ell} - 2r^{L-\ell}r^\ell - \sqrt{2} \sum_{k=\ell+1}^L r^{L-\ell-1+\frac{k-1}{2}} \\ &= \Theta_\infty^{(L)}(x, x) - 2Lr^L - \sqrt{2} \sum_{\ell=1}^L r^{L-\frac{\ell}{2}-1} \sum_{k=0}^{L-\ell-1} r^{\frac{k}{2}} \\ &\geq \Theta_\infty^{(L)}(x, x) - 2Lr^L - \frac{\sqrt{2}}{1-\sqrt{r}} r^{L/2-1} \sum_{\ell=0}^{L-1} r^{\ell/2} \\ &= \Theta_\infty^{(L)}(x, x) - 2Lr^L - \frac{\sqrt{2}}{1-\sqrt{r}} r^{L/2-1} \frac{1}{1-\sqrt{r}} \\ &\geq \Theta_\infty^{(L)}(x, x) - 2Lr^L - \frac{\sqrt{2}}{(1-\sqrt{r})^2} r^{L/2-1} \\ &\geq \Theta_\infty^{(L)}(x, x) - \left[ 2Lr^{L/2} - \frac{\sqrt{2}}{r(1-\sqrt{r})^2} \right] r^{L/2} \\ &\geq \Theta_\infty^{(L)}(x, x) - C_0(r, \beta)r^{L/2}. \end{aligned}$$

Recall that for any  $x \in \mathbb{S}_{n_0}$ ,  $\Theta_\infty^{(L)}(x, x) = \frac{1-r^L}{1-r}$  is bounded in  $L$ . Dividing the previous inequality by  $\Theta_\infty^{(L)}(x, x)$  we get:  $1 - Cr^{L/2} \leq \vartheta_L(x, y) \leq 1$ .  $\square$

## C Layer Normalization and Nonlinearity Normalization

With Layer Normalization (LN), the normalized vector of activations is  $\check{\alpha}^{(\ell)}(x) = \frac{\alpha^{(\ell)}(x) - \frac{1}{n_\ell} \sum_{i=1}^{n_\ell} \alpha_i^{(\ell)}(x)}{\|\alpha^{(\ell)}(x) - \frac{1}{n_\ell} \sum_{i=1}^{n_\ell} \alpha_i^{(\ell)}(x)\|}$ . As a consequence, at initialization, all pre-activations—except the

ones of the first hidden layer—have variance 1:

$$\mathbb{E} \left[ \left( \sqrt{\frac{1-\beta^2}{n_\ell}} W_i^{(\ell)} \tilde{\alpha}^{(\ell)}(x) + \beta b_i^{(\ell)} \right)^2 \right] = \frac{1-\beta^2}{n_\ell} \left\| \tilde{\alpha}^{(\ell)}(x) \right\|^2 + \beta^2 = 1.$$

The pre-activations of the first hidden layer have variance  $\frac{1-\beta^2}{n_0} \|x\|^2 + \beta^2$  which is equal to 1 under the assumption that  $x$  lies on  $\mathbb{S}_{n_0}$ .

As a consequence, using the same arguments which were used to prove the convergence of the activation kernels, as  $n_1, \dots, n_\ell \rightarrow \infty$  sequentially, the mean that is subtracted converges:

$$\frac{1}{n_\ell} \sum_i \alpha_i^{(\ell)}(x) \rightarrow \mathbb{E}_{x \sim \mathcal{N}(0,1)} [\sigma(x)].$$

Furthermore, during training, using the arguments of [12], one could in principle prove that the preactivations  $\tilde{\alpha}_i^{(\ell)}(x)$  change at a rate of  $1/\sqrt{n_\ell}$ , which induce a total change of  $\frac{1}{n_\ell} \sum_i \alpha_i^{(\ell)}(x)$  of the same rate: it should be asymptotically deterministic and fixed.

Similarly, the variance converges to a deterministic and fixed value:

$$\begin{aligned} \frac{1}{\sqrt{n_\ell}} \left\| \alpha^{(\ell)}(x) - \frac{1}{n_\ell} \sum_i \alpha_i^{(\ell)}(x) \right\|^2 &= \frac{1}{\sqrt{n_\ell}} \sum_j \left( \alpha_j^{(\ell)}(x) - \frac{1}{n_\ell} \sum_i \alpha_i^{(\ell)}(x) \right)^2 \\ &\rightarrow \mathbb{E} \left[ (\sigma(x) - \mathbb{E}[\sigma(x)])^2 \right]. \end{aligned}$$

Thus, LN is asymptotically equivalent to centering and standardizing the non-linearity.

## D Batch Normalization

If one adds a BatchNorm layer after the non-linearity of the last hidden layer, we have:

**Lemma 1.** Consider FC-NN with  $L$  layers, with a PN-BN after the last nonlinearity, for any  $k, k' \in \{1, \dots, n_L\}$  and any parameter  $\theta_p$ , we have  $\sum_{i=1}^N \Theta_{\theta_p}^{(L)}(\cdot, x_i) = \beta^2 \text{Id}_{n_L}$ .

*Proof.* This is an direct consequence of the definition of the NTK and of the following claim:

**Claim 1.** For a fully-connected DNN with a BatchNorm layer after the non-linearity of the last hidden layer then  $\frac{1}{N} \sum_{i=1}^N \partial_{\theta_p} f_{\theta, k}(x_i)$  is equal to  $\beta$  if  $\theta_p$  is  $b_k^{(L-1)}$ , the bias parameter of the last layer, and equal to 0 otherwise.

The average of  $f_{\theta, k}$  on the training set,  $\frac{1}{N} \sum_{i=1}^N \partial_{\theta_p} f_{\theta, k}(x_i)$ , only depends on the bias of the last layer:

$$\frac{1}{N} \sum_{i=1}^N f_{\theta, k}(x_i) = \frac{\sqrt{1-\beta^2}}{\sqrt{n_{L-1}}} W^{(L-1)} \frac{1}{N} \sum_{i=1}^N \hat{\alpha}^{(L-1)}(x_i) + \beta b_k^{(L-1)} = \beta b_k^{(L-1)}.$$

Thus for any parameter  $\theta_p$ ,  $\frac{1}{N} \sum_{i=1}^N \partial_{\theta_p} f_{\theta, k}(x_i) = \partial_{\theta_p} (\beta b_k^{(L-1)})$  is equal to  $\beta$  if the parameter is the bias  $b_k^{(L-1)}$  and zero otherwise.  $\square$

## E General Convolutional Networks

In this section, we prove the convergence of the NTK at initialization for a general family of DNNs which contain in particular CNNs and DC-NNs. We will consider the parent-based parametrization introduced in Section 6.

For each layer  $\ell = 0, \dots, L$ , the neurons are indexed by a position  $p \in I_\ell$  and a channel  $i = 1, \dots, n_\ell$ . We may assume that the sets of positions  $I_\ell$  can be any set, in particular any subset of  $\mathbb{Z}^D$ . For



any position  $p \in I_{\ell+1}$ , we consider a set of parents  $P(p) \subset I_\ell$  and we define recursively the set  $P^{\circ k}(p) \subset I_{\ell+1-k}$  of ancestors of level  $k$  by  $P^{\circ k}(p) = \{q \mid \exists q' \in P^{\circ k-1}(p), q \in P(q')\}$ . For each parent  $q \in P(p)$ , the connections from the position  $(q, \ell)$  to the position  $(p, \ell+1)$  are encoded in an  $n_\ell \times n_{\ell+1}$  weight matrix  $W^{(\ell, q \rightarrow p)}$ . We define  $\chi(q \rightarrow p, q' \rightarrow p')$  which is equal to 1 if and only if  $W^{(\ell, q \rightarrow p)}$  and  $W^{(\ell, q' \rightarrow p')}$  are shared (in the sense that the two matrices are forced to be equal at initialization and during training) and 0 otherwise. It satisfies  $\chi(q \rightarrow p, q \rightarrow p) = 1$  for any neuron  $p$  and any  $q \in P(p)$  and it is transitive. We will also suppose that for any neuron  $p$  and any  $q, q' \in P(p)$ ,  $\chi(q \rightarrow p, q' \rightarrow p) = \delta_{qq'}$  (i.e. no pair of connections connected to the same neuron  $p$  are shared).

In this setting, the activations and preactivations  $\alpha^{(\ell)}, \tilde{\alpha}^{(\ell)} \in (\mathbb{R}^{n_\ell})^{I_\ell}$  are recursively constructed using the parent-based NTK parametrization: we set  $\alpha^{(0)}(x) = x$  and for  $\ell = 0, \dots, L-1$  and any position  $p \in I_\ell$ :

$$\tilde{\alpha}^{(\ell+1, p)}(x) = \beta b^{(\ell)} + \frac{\sqrt{1-\beta^2}}{\sqrt{|P(p)|} n_\ell} \sum_{q \in P(p)} W^{(\ell, q \rightarrow p)} x_q, \quad \alpha^{(\ell+1)}(x) = \sigma \left( \tilde{\alpha}^{(\ell+1)}(x) \right)$$

where  $\sigma$  is applied entry-wise,  $\beta \geq 0$  and  $|P(p)|$  is the cardinal of  $P(p)$ . This is a slightly more general formalism than the DC-NNs and it will allow us to obtain simpler formulae which generalize well to other architectures.

**Remark 3.** Notice that the parametrization is slightly different than the one introduced in Section 2.2: we divided by  $\sqrt{|P(p)|} n_\ell$  instead of dividing by  $\sqrt{n_\ell^{|\omega|/s_1 \dots s_d}}$ . This does not lead to any difference when one consider infinite-sized images as in Section F since in this case the number of parents is constant, equal to  $|\omega|/s_1 \dots s_d$ . The key difference between the two parametrizations will be investigated in Section G.

For a kernel matricial kernel  $K : \mathbb{R}^{n_0} \times \mathbb{R}^{n_0} \rightarrow \mathbb{R}^{I_\ell} \otimes \mathbb{R}^{I_\ell}$ , for any  $z_0, z_1 \in \mathbb{R}^{n_0}$  and any  $p_0, p_1 \in I_\ell$ , we define:

$$\mathbb{L}_{K, p_0 p_1}^g(z_0, z_1) = \mathbb{E}_{(y_0, y_1) \sim \mathcal{N}(0, (K_{p_i, p_j}(z_i, z_j))_{i, j=0,1})} [g(y_0) g(y_1)].$$

**Proposition 4.** In this setting, as  $n_1 \rightarrow \infty, \dots, n_{\ell-1} \rightarrow \infty$  sequentially, the preactivations  $(\tilde{\alpha}_i^{(\ell, p)}(x))_{i=1, \dots, n_\ell, p \in I_\ell}$  of the  $\ell^{\text{th}}$  layer converge to a centered Gaussian process with covariance  $\Sigma_{pp'}^{(\ell)}(x, y) \delta_{ii'}$ , where  $\Sigma_{pp'}^{(\ell)}(x, y)$  is defined recursively as

$$\begin{aligned} \Sigma_{pp'}^{(1)}(x, y) &= \beta^2 + \frac{1-\beta^2}{\sqrt{|P(p)|} |P(p')| n_0} \sum_{q \in P(p)} \sum_{q' \in P(p')} \chi(q \rightarrow p, q' \rightarrow p') (x_q)^T y_{q'}, \\ \Sigma_{pp'}^{(\ell+1)}(x, y) &= \beta^2 + \frac{1-\beta^2}{\sqrt{|P(p)|} |P(p')|} \sum_{q \in P(p)} \sum_{q' \in P(p')} \chi(q \rightarrow p, q' \rightarrow p') \mathbb{L}_{\sigma, qq'}^{\Sigma_{\sigma, qq'}^{(\ell)}}(x, y). \end{aligned}$$

*Proof.* The proof is done by induction on  $\ell$ . For  $\ell = 1$  and any  $i \in \{1, \dots, n_1\}$ , the preactivation

$$\tilde{\alpha}_i^{(1, p)}(x) = \beta b_i^{(0)} + \frac{\sqrt{1-\beta^2}}{\sqrt{|P(p)|} n_0} \sum_{q \in P(p)} \left( W_p^{(0, q \rightarrow p)} x_q \right)_i$$

is a random affine function of  $x$  and its coefficients are centered Gaussian: it is hence a centered Gaussian process whose covariance is easily shown to be equal to  $\mathbb{E} \left[ \tilde{\alpha}_i^{(1, p)}(x) \tilde{\alpha}_{i'}^{(1, p')}(y) \right] = \Sigma_{pp'}^{(1)}(x, y) \delta_{ii'}$ .

For the induction step, we assume that the result holds for the pre-activations of the layer  $\ell$ . The pre-activations of the next layer are of the form

$$\tilde{\alpha}_i^{(\ell+1, p)}(x) = \beta b_i^{(0)} + \frac{\sqrt{1-\beta^2}}{\sqrt{|P(p)|} n_\ell} \sum_{q \in P(p)} \left( W^{(\ell, q \rightarrow p)} \alpha^{(\ell, q)}(x) \right)_i.$$

Conditioned on the activations  $\alpha^{(\ell,q)}$  of the last layer,  $\tilde{\alpha}^{(\ell+1,p)}$  is a centered Gaussian process: in other terms, it is a mixture of centered Gaussians with a random covariance determined by the activations of the last layer. The random covariance between  $\tilde{\alpha}_{i_0}^{(\ell+1,p_0)}(x)$  and  $\tilde{\alpha}_{i_1}^{(\ell+1,p_1)}(y)$  is equal to

$$\begin{aligned} & \beta^2 \delta_{i_0 i_1} + \frac{1 - \beta^2}{\sqrt{|P(p_0)||P(p_1)|}^{n_\ell}} \sum_{\substack{q_0 \in P(p_0) \\ q_1 \in P(p_1)}} \sum_{j_0, j_1=1}^{n_\ell} \mathbb{E} \left[ W_{i_0 j_0}^{(\ell, q_0 \rightarrow p_0)} W_{i_1 j_1}^{(\ell, q_1 \rightarrow p_1)} \right] \alpha_{j_0}^{(\ell, q_0)}(x) \alpha_{j_1}^{(\ell, q_1)}(y) \\ &= \delta_{i_0 i_1} \left[ \beta^2 + \frac{1 - \beta^2}{\sqrt{|P(p_0)||P(p_1)|}^{n_\ell}} \sum_{\substack{q_0 \in P(p_0) \\ q_1 \in P(p_1)}} \chi(q_0 \rightarrow p_0, q_1 \rightarrow p_1) \frac{1}{n_\ell} \sum_{j=1}^{n_\ell} \sigma \left( \tilde{\alpha}_j^{(\ell, q_0)}(x) \right) \sigma \left( \tilde{\alpha}_j^{(\ell, q_1)}(y) \right) \right], \end{aligned}$$

where we used the fact that  $\mathbb{E} \left[ W_{i_0 j_0}^{(\ell, q_0 \rightarrow p_0)} W_{i_1 j_1}^{(\ell, q_1 \rightarrow p_1)} \right] = \chi(q_0 \rightarrow p_0, q_1 \rightarrow p_1) \delta_{i_0 i_1} \delta_{j_0 j_1}$ . Using the induction hypothesis, as  $n_1 \rightarrow \infty, \dots, n_{\ell-1} \rightarrow \infty$  sequentially, the preactivations  $\left( \tilde{\alpha}_j^{(\ell, q_0)}(x), \tilde{\alpha}_j^{(\ell, q_1)}(y) \right)_j$  converge to independant centered Gaussian pairs. As  $n_\ell \rightarrow \infty$ , by the law of large numbers, the sum over  $j$  along with the  $1/n_\ell$  converges to  $\mathbb{L}_{\sigma, qq'}^{\Sigma^{(\ell)}}(x, y)$ . In this limit, the random covariance of the Gaussian mixture becomes deterministic and as a consequence, the mixture of Gaussian processes tends to a centered Gaussian process with the right covariance.  $\square$

Similarly to the activation kernels, one can prove that the NTK converges at initialization.

**Proposition 5.** *As  $n_1 \rightarrow \infty, \dots, n_{L-1} \rightarrow \infty$  sequentially, the NTK  $\Theta_{p_0 p_1}^{(L)}$  of a general convolutional network converges to  $\Theta_{\infty, p_0 p_1}^{(L)} \otimes \text{Id}_{n_L}$  where  $\Theta_{\infty, p_0 p_1}^{(L)}(x, y)$  is defined recursively by:*

$$\begin{aligned} \Theta_{\infty, p_0 p_1}^{(1)}(x, y) &= \Sigma_{p_0 p_1}^{(1)}(x, y), \\ \Theta_{\infty, p_0 p_1}^{(L)}(x, y) &= \frac{1 - \beta^2}{\sqrt{|P(p_0)||P(p_1)|}^{n_L}} \sum_{\substack{q_0 \in P(p_0) \\ q_1 \in P(p_1)}} \chi(q_0 \rightarrow p_0, q_1 \rightarrow p_1) \Theta_{\infty, q_0 q_1}^{(L-1)}(x, y) \mathbb{L}_{\sigma, q_0 q_1}^{\Sigma^{(L-1)}}(x, y) \\ &\quad + \Sigma_{p_0 p_1}^{(L)}(x, y). \end{aligned}$$

*Proof.* The proof by induction on  $L$  follows the one of [12] for fully-connected DNNs. We present the induction step and assume that the result holds for a general convolutional network with  $L - 1$  hidden layers. Following the same computations as in [12], the NTK  $\Theta_{p_0 p_1, j j'}^{(L+1)}(x, y)$  is equal to

$$\begin{aligned} & \frac{1 - \beta^2}{\sqrt{|P(p_0)||P(p_1)|}^{n_L}} \sum_{q_0 \in P(p_0)} \sum_{q_1 \in P(p_1)} \sum_{ii'} \Theta_{q_0 q_1, ii'}^{(L)}(x, y) \dot{\sigma} \left( \tilde{\alpha}_i^{(L, q_0)}(x) \right) \dot{\sigma} \left( \tilde{\alpha}_{i'}^{(L, q_1)}(y) \right) \\ & \quad W_{ij}^{(L, q_0 \rightarrow p_0)} W_{i' j'}^{(L, q_1 \rightarrow p_1)} \\ & + \delta_{j j'} \beta^2 + \delta_{j j'} \frac{1 - \beta^2}{\sqrt{|P(p_0)||P(p_1)|}^{n_L}} \sum_{q_0 \in P(p_0)} \sum_{q_1 \in P(p_1)} \chi(q_0 \rightarrow p_0, q_1 \rightarrow p_1) \sum_i \alpha_i^{(L, q_0)}(x) \alpha_i^{(L, q_1)}(y) \end{aligned}$$

which, by assumption, converges as  $n_1 \rightarrow \infty, \dots, n_{L-1} \rightarrow \infty$  to

$$\begin{aligned} & \frac{1 - \beta^2}{\sqrt{|P(p_0)||P(p_1)|}^{n_L}} \sum_{q_0 \in P(p_0)} \sum_{q_1 \in P(p_1)} \sum_i \Theta_{\infty, q_0 q_1}^{(L)}(x, y) \dot{\sigma} \left( \tilde{\alpha}_i^{(L, q_0)}(x) \right) \dot{\sigma} \left( \tilde{\alpha}_i^{(L, q_1)}(y) \right) \\ & \quad W_{ij}^{(L, q_0 \rightarrow p_0)} W_{i' j'}^{(L, q_1 \rightarrow p_1)} \\ & + \delta_{j j'} \beta^2 + \delta_{j j'} \frac{1 - \beta^2}{\sqrt{|P(p_0)||P(p_1)|}^{n_L}} \sum_{q_0 \in P(p_0)} \sum_{q_1 \in P(p_1)} \chi(q_0 \rightarrow p_0, q_1 \rightarrow p_1) \sum_i \alpha_i^{(L, q_0)}(x) \alpha_i^{(L, q_1)}(y). \end{aligned}$$

As  $n_L \rightarrow \infty$ , using the previous results on the preactivations and the law of large number, the NTK converges to

$$\begin{aligned} & \frac{1 - \beta^2}{\sqrt{|P(p_0)||P(p_1)|}} \sum_{q_0 \in P(p_0)} \sum_{q_1 \in P(p_1)} \Theta_{\infty, q_0 q_1}^{(L)}(x, y) \mathbb{L}_{\hat{\sigma}}^{\Sigma_{q_0 q_1}^{(L)}}(x, y) \mathbb{E} \left[ W_{ij}^{(L, q_0 \rightarrow p_0)} W_{ij'}^{(L, q_1 \rightarrow p_1)} \right] \\ & + \delta_{jj'} \beta^2 + \delta_{jj'} \frac{1 - \beta^2}{\sqrt{|P(p_0)||P(p_1)|}} \sum_{q_0 \in P(p_0)} \sum_{q_1 \in P(p_1)} \chi(q_0 \rightarrow p_0, q_1 \rightarrow p_1) \mathbb{L}_{\hat{\sigma}, q_0 q_1}^{\Sigma_{q_0 q_1}^{(L)}}(x, y), \end{aligned}$$

which can be simplified—using the fact that  $\mathbb{E} \left[ W_{ij}^{(L, q_0 \rightarrow p_0)} W_{ij'}^{(L, q_1 \rightarrow p_1)} \right] = \chi(q_0 \rightarrow p_0, q_1 \rightarrow p_1) \delta_{jj'}$ —into:

$$\begin{aligned} & \delta_{jj'} \frac{1 - \beta^2}{\sqrt{|P(p_0)||P(p_1)|}} \sum_{q_0 \in P(p_0)} \sum_{q_1 \in P(p_1)} \chi(q_0 \rightarrow p_0, q_1 \rightarrow p_1) \Theta_{\infty, q_0 q_1}^{(L)}(x, y) \mathbb{L}_{\hat{\sigma}, q_0 q_1}^{\Sigma_{q_0 q_1}^{(L)}}(x, y) \\ & + \delta_{jj'} \Sigma_{p_0 p_1}^{\Sigma_{p_0 p_1}^{(L+1)}}(x, y), \end{aligned}$$

which proves the assertions.  $\square$

## F DC-NN Freeze and Chaos

In this section, in order to study the behaviour of DC-NNs in the bulk and to avoid dealing with border effects, studied in Section G, we assume that for all layers  $\ell$  there is no border, i.e. the positions  $p$  are in  $\mathbb{Z}^d$ . Let us consider a DC-NN with up-sampling  $s \in \{2, 3, \dots\}^d$  where the window sizes for all layers are all set equal to  $\pi = \omega = \{0, \dots, w_1 s_1 - 1\} \times \dots \times \{0, \dots, w_d s_d - 1\}$ . A position  $p$  has therefore  $w_1 \cdot \dots \cdot w_d$  parents which are given by

$$P(p) = \{ \lfloor p_0/s_0 \rfloor, \lfloor p_0/s_0 \rfloor + 1, \dots, \lfloor p_0/s_0 \rfloor + w_0 \} \times \dots \times \{ \lfloor p_d/s_d \rfloor, \lfloor p_d/s_d \rfloor + 1, \dots, \lfloor p_d/s_d \rfloor + w_d \}.$$

Two connections  $q \rightarrow p$  and  $q' \rightarrow p'$  are shared if and only if  $s \mid p - p'$  (i.e. for any  $i = 1, \dots, d$ ,  $s_i \mid p_i - p'_i$ ) and  $q_i - q'_i = \frac{p_i - p'_i}{s_i}$  for any  $i = 1, \dots, d$ .

Propositions 4 and 5 hold true in this setting. By Proposition 2, if the non-linearity  $\sigma$  is standardized,  $\Sigma_{pp}^{(\ell)}(x, x) = 1$  for any  $x \in \mathbb{S}_{n_0}^{I_0}$  and any  $p \in I_\ell$ . The activation kernels  $\Sigma_{p, p'}^{(\ell)}(x, y)$  for any two inputs  $x, y \in \mathbb{S}_{n_0}^{I_0}$  and two output positions  $p, p' \in \mathbb{Z}^d$  are therefore defined recursively by:

$$\begin{aligned} \Sigma_{pp'}^{(1)}(x, y) &= \beta^2 + \delta_{s \mid p - p'} \frac{1 - \beta^2}{|P(p)| n_0} \sum_{q \in P(p)} (x_q)^T y_{q + \frac{p' - p}{s}}, \\ \Sigma_{pp'}^{(\ell+1)}(x, y) &= \beta^2 + \delta_{s \mid p - p'} \frac{1 - \beta^2}{|P(p)|} \sum_{q \in P(p)} R_\sigma \left( \Sigma_{q, q + \frac{p' - p}{s}}^{(\ell)}(x, y) \right), \end{aligned}$$

where  $\frac{p' - p}{s} = \left( \frac{p'_i - p_i}{s_i} \right)_i$  is a valid position since  $s \mid p - p'$ . Similarly, the NTK at initialization satisfies the following recursion:

$$\Theta_{\infty, pp'}^{(L+1)}(x, y) = \Sigma_{pp'}^{(L+1)}(x, y) + \delta_{s \mid p - p'} \frac{1 - \beta^2}{|P(p)|} \sum_{q \in P(p)} \Theta_{\infty, q, q + \frac{p' - p}{s}}^{(L)}(x, y) R_{\hat{\sigma}} \left( \Sigma_{q, q + \frac{p' - p}{s}}^{(L)}(x, y) \right).$$

**Remark 4.** Recall that the  $s$ -valuation  $v_s(n)$  of a number  $n \in \mathbb{Z}^d$  is the largest  $k \in \{0, 1, 2, \dots\}$  such that  $s_i^k \mid n_i$  for all dimensions  $i = 1, \dots, d$ . For two pixels  $p, p' \in \mathbb{Z}^d$  and any input vectors  $x, y \in \mathbb{S}_{n_0}^{I_0}$ , if  $v_s(p' - p) < \ell$  the activation kernel  $\Sigma_{pp'}^{(\ell)}(x, y)$  does not depend neither on  $x$  nor on  $y$ . More precisely, if  $v = v_s(p' - p) = 0$ , we have

$$\Sigma_{pp'}^{(\ell)}(x, y) = \beta^2,$$

and for a general  $v < \ell$ :

$$c_v := \Sigma_{pp'}^{(\ell)}(x, y) = (B_\beta \circ R_\sigma)^{\circ v}(\beta^2).$$

In particular, if  $v < L$ , the NTK is therefore also equal to a constant:

$$\Theta_{pp'}^{(L)}(x, y) = \sum_{k=0}^v c_k (1 - \beta^2)^k \prod_{m=0}^{k-1} R_{\dot{\sigma}}(c_m).$$

We establish the bounds on the rate of convergence in the ‘‘freeze’’ region and on the values of the activations kernel in the chaos region for DC-NNs.

**Proposition 6.** *In the setting introduced above, for a standardized twice differentiable  $\sigma$ , for  $x, y \in \mathbb{S}_{n_0}^{I_0}$ , and any positions  $p, p' \in I_\ell$ , taking  $k = \min\{v_s(p' - p), \ell\}$ , we have:*

If  $r_{\sigma, \beta} < 1$  then:

$$1 \geq \Sigma^{(\ell, pp')}(x, y) \geq 1 - 2(1 - \beta^2)r_{\sigma, \beta}^k.$$

If  $r_{\sigma, \beta} > 1$  then there exists a fixed point  $a \in [0, 1)$  of  $B_\beta \circ R_\sigma$  such that:

- If  $k < \ell$ :

$$\left| \Sigma^{(\ell, pp')}(x, y) \right| \leq \max\{\beta^2, a\},$$

- If  $p' - p = ms^\ell$  and there is a  $c \leq 1$  such that for all input positions  $q \in P^{\circ \ell}(p)$ ,  $\left| \frac{1}{n_0} x_q^T y_{q+m} \right| \leq c$ , then

$$\left| \Sigma^{(\ell, pp')}(x, y) \right| \leq \max\{\beta^2 + (1 - \beta^2)c, a\}.$$

*Proof.* Let us denote  $r = r_{\sigma, \beta}$ . Let us suppose that  $r < 1$  and let us prove the first assertion by induction on  $\ell$ . If  $\ell = 1$ , then

$$\begin{aligned} \Sigma^{(1, pp')}(x, y) &= \beta^2 + \delta_{s|p-p'} \frac{1 - \beta^2}{|P(p)| n_0} \sum_{q \in P(p)} (x_q)^T y_{q + \frac{p'-p}{s}} \\ &\geq \beta^2 - \delta_{s|p-p'} (1 - \beta^2) \\ &\geq 1 - 2(1 - \beta^2) \end{aligned}$$

For the induction step, if we suppose that the inequality holds true for  $\ell$ , then

$$\begin{aligned} \Sigma^{(\ell+1, pp')}(x, y) &\geq \beta^2 + \delta_{s|p-p'} \frac{1 - \beta^2}{|P(p)|} \sum_{q=0}^{w/s} R_\sigma(1 - 2(1 - \beta^2)r^{k-1}) \\ &\geq \beta^2 + \delta_{s|p-p'} \frac{1 - \beta^2}{|P(p)|} \sum_{q=0}^{w/s} 1 - 2(1 - \beta^2)R_{\dot{\sigma}}(1)r^{k-1} \\ &\geq \beta^2 + \delta_{s|p-p'} (1 - \beta^2 - 2(1 - \beta^2)r^k) \\ &= \begin{cases} 1 - (1 - \beta^2) & \text{if } k = 0 \\ 1 - 2(1 - \beta^2)r^k & \text{if } k > 0 \end{cases} \\ &\geq 1 - 2(1 - \beta^2)r^k \end{aligned}$$

Now let us suppose that  $r > 1$ . If  $k < \ell$ , then  $\left| \Sigma^{(\ell, pp')}(x, y) \right| = \left| (B_\beta \circ R_\sigma)^{\circ k}(\beta^2) \right| < \max\{\beta^2, a\}$ . Let us suppose at last that  $k = \ell$  and let us prove the last assertion by induction on  $\ell$ . If  $\ell = 1$ , then

$$\begin{aligned} \left| \Sigma^{(1, pp')}(x, y) \right| &\leq \beta^2 + \frac{1 - \beta^2}{|P(p)| n_0} \sum_{q \in P(p)} \left| x_q^T y_{q + \frac{p'-p}{s}} \right| \\ &\leq \beta^2 + \frac{1 - \beta^2}{|P(p)|} \sum_{q \in P(p)} c \\ &= \beta^2 + (1 - \beta^2)c. \end{aligned}$$

For the induction step, if we suppose that the inequality holds true for  $\ell$ , then

$$\begin{aligned}
\left| \Sigma^{(\ell+1, pp')}(x, y) \right| &\leq \beta^2 + \frac{(1-\beta^2)}{|P(p)|} \sum_{q \in P(p)} \left| R_\sigma \left( \Sigma^{(\ell, q, q + \frac{p'-p}{s})(x, y)} \right) \right| \\
&\leq \beta^2 + \frac{(1-\beta^2)}{|P(p)|} \sum_{q \in P(p)} R_\sigma \left( \max\{\beta^2 + (1-\beta^2)c, a\} \right) \\
&= B_\beta \circ R_\sigma \left( \max\{\beta^2 + (1-\beta^2)c, a\} \right) \\
&\leq \max\{\beta^2 + (1-\beta^2)c, a\},
\end{aligned}$$

which allow us to conclude.  $\square$

The NTK features the same two regimes:

**Theorem 4.** Take  $I_0 = \mathbb{Z}^d$ , and consider a DC-NN with upsampling stride  $s \in \{2, 3, \dots\}^d$ , windows  $\pi_\ell = \omega_\ell = \{0, \dots, w_1 s_1 - 1\} \times \dots \times \{0, \dots, w_d s_d - 1\}$  for  $w \in \{1, 2, 3, \dots\}^d$ . For a standardized twice differentiable  $\sigma$ , there exist constants  $C_1, C_2 > 0$ , such that the following holds: for  $x, y \in \mathbb{S}_{n_0}^{I_0}$ , and any positions  $p, p' \in I_L$ , we have:

**Freeze:** When  $r_{\sigma, \beta} < 1$ , taking  $v = \min(v_s(p-p'), L-1)$ , taking  $v = L-1$  if  $p = p'$  and  $r = r_{\sigma, \beta}$ , we have

$$\frac{1-r^{v+1}}{1-r^L} - C_1(v+1)r^v \leq \vartheta_{p, p'}^{(L)}(x, y) \leq \frac{1-r^{v+1}}{1-r^L}.$$

**Chaos:** When  $r_{\sigma, \beta} > 1$ , if either  $v_s(p-p') < L$  or if there exists a  $c < 1$  such that for all positions  $q \in I_0$  which are ancestor of  $p$ ,  $\left| x_q^T y_{q + \frac{p'-p}{s}} \right| < c$ , then there exists  $h < 1$  such that

$$\left| \vartheta_{p, p'}^{(L)}(x, y) \right| \leq C_2 h^L.$$

*Proof.* Let us denote  $r = r_{\sigma, \beta}$  and let us suppose that  $r < 1$ . The NTK can be bounded recursively

$$\begin{aligned}
\Theta_{pp'}^{(L)}(x, y) &= \Sigma^{(L, pp')}(x, y) + \delta_{s|p-p'} \frac{1-\beta^2}{|P(p)|} \sum_{q \in P(p)} \Theta_\infty^{(L-1; q, q + \frac{p'-p}{s})}(x, y) R_\sigma \left( \Sigma^{(L-1; q, q + \frac{p'-p}{s})}(x, y) \right) \\
&\geq 1 - 2(1-\beta^2)r^v + \delta_{s|p-p'} \frac{1}{|P(p)|} \sum_{q \in P(p)} \Theta_\infty^{(L; q, q + \frac{p'-p}{s})}(x, y) (r - \psi 2(1-\beta^2)^2 r^{v-1}).
\end{aligned}$$

Unrolling this inequality, we get:

$$\begin{aligned}
\Theta_{pp'}^{(L)}(x, y) &= \sum_{k=0}^v (1 - 2(1-\beta^2)r^k) \prod_{m=k+1}^v (r - \psi 2(1-\beta^2)^2 r^{m-1}) \\
&\geq \sum_{k=0}^v r^{v-k} - 2(1-\beta^2)r^{v-k}r^k - \psi 2(1-\beta^2)^2 \sum_{m=k+1}^v r^{v-k-1}r^{m-1} \\
&= \frac{1-r^{v+1}}{1-r} - 2(1-\beta^2)(v+1)r^v - \psi 2(1-\beta^2)^2 \sum_{k=0}^v r^{v-1} \sum_{m=0}^{v-k-1} r^m \\
&\geq \frac{1-r^{v+1}}{1-r} - 2(1-\beta^2) \left[ r + \frac{\psi(1-\beta^2)}{1-r} \right] (v+1)r^{v-1} \\
&\geq \frac{1-r^{v+1}}{1-r} - C_{\sigma, \beta}(v+1)r^v.
\end{aligned}$$

For the upper bound, we have:  $\Theta_{pp'}^{(L)}(x, y) \leq \sum_{\ell=L-k}^L 1 \prod_{m=\ell+1}^L r = \frac{1-r^{v+1}}{1-r}$ . Thus, we get the same bounds as in the FC-NNs case, but with respect to  $v$ , which is the maximal integer strictly smaller than  $L$  such that  $s^v|p-p'$ :

$$\frac{1-r^{v+1}}{1-r} \geq \Theta_{pp'}^{(L)}(x, y) \geq \frac{1-r^{v+1}}{1-r} - C(v+1)r^v.$$

Dividing by  $\Theta_{pp}^{(L)}(x, x)$  which is bounded in the frozen regime (see proof of Proposition 2) as  $L \rightarrow \infty$ , one gets the desired result.

If  $r > 1$ , there are two cases. When  $p' - p = ks^L$  then if there exists  $c < 1$  such that  $|x_q^T y_{q+k}| < cn_0$  for all ancestors  $q$  of  $p$ . Writing  $z = \max\{\beta^2 + (1 - \beta^2)c, a\}$  and  $w = (1 - \beta^2)R_{\hat{\sigma}}(z) < r$  such that  $|\Sigma^{(\ell; q, q+ks^\ell)}(x, y)| < z$  for all position  $q$  at layer  $\ell$  which is an ancestor of  $p$ . Then

$$\left| \Theta_{pp'}^{(L)}(x, y) \right| \leq \sum_{\ell=1}^L vw^{L-\ell} = v \frac{1-w^L}{1-w}$$

such that

$$\frac{\left| \Theta_{pp'}^{(L)}(x, y) \right|}{\left| \Theta_{pp}^{(L)}(x, x) \right|} \leq c \frac{1-r}{1-w} \frac{1-w^L}{1-r^L} \leq C(\sigma, \beta) \left( \frac{w}{r} \right)^L$$

which goes to zero exponentially.

If  $p' - p$  is not divisible by  $s^L$  then for  $z = \max\{\beta^2, a\}$  and  $w = (1 - \beta^2)R_{\hat{\sigma}}(z) < r$

$$\left| \Theta_{pp'}^{(L)}(x, y) \right| \leq \sum_{\ell=L-v+1}^L zw^{L-\ell} = z \frac{1-w^v}{1-w}$$

which also converges exponentially to 0. □

## F.1 Adapting the learning rate

Let us suppose that we multiply the learning rate of the  $\ell$ -th layer weights and bias by  $S^{-\frac{\ell}{2}}$  where  $S = \prod_i s_i$ . This is slightly different than what we propose in Section 6.1, where the learning rate of the bias are multiplied by  $S^{-\frac{\ell+1}{2}}$  instead of  $S^{-\frac{\ell}{2}}$ , but it greatly simplifies the formulas. Furthermore, the balance between the weights and bias can be modified with the meta-parameter  $\beta$  to achieve a similar result. The NTK then takes the value:

$$\begin{aligned} \Theta_{pp}^{(L)}(x, x) &= \sum_{\ell=1}^L S^{-\frac{\ell}{2}} \prod_{n=\ell+1}^L r \\ &= \sum_{\ell=1}^L S^{-\frac{\ell}{2}} r^{L-\ell} \\ &= \sum_{\ell=0}^{L-1} S^{-\frac{L-\ell}{2}} r^\ell \\ &= S^{-\frac{L}{2}} \frac{1 - (\sqrt{Sr})^L}{1 - \sqrt{Sr}} \end{aligned}$$

This leads to another transtion inside the “freeze” regime: if  $\sqrt{Sr} < 1$  the NTK  $\Theta_{pp}^{(L)}(x, x)$  goes to zero and if  $\frac{1}{\sqrt{S}} < r < 1$  it converges to a constant. If we translate the bound of Proposition 4 to the NTK with varying learning rates, the convergence to a constant is only guaranteed when  $\sqrt{Sr} < 1$ , which suggests that adapting the learning (or changing the number of channels) does reduce the checkerboard artifacts (as confirmed by numerical experiments):

**Proposition 7.** *If  $r < 1$  the limiting NTK at any two inputs  $x, y$  such that for all  $p \in \mathbb{Z}$ ,  $\|x^p\| = \|y^p\| = \sqrt{n_0}$  and for any two output positions  $p$  and  $p'$ , such that  $k$  is the maximal integer in  $\{0, \dots, L-1\}$  such that  $s^k$  divides the difference  $p - p'$  then:*

$$\frac{1 - (\sqrt{Sr})^{k+1}}{1 - (\sqrt{Sr})^L} \geq \Theta_{pp'}^{(L)}(x, y) \geq \frac{1 - (\sqrt{Sr})^{k+1}}{1 - (\sqrt{Sr})^L} - \frac{C_{\sigma, \beta}(\sqrt{Sr})^k}{|1 - (\sqrt{Sr})^L|}$$

*Proof.* The NTK can be bounded recursively

$$\begin{aligned}\Theta_{pp'}^{(L)}(x, y) &= S^{-L-1/2} \Sigma^{(L, pp')}(x, y) + \delta_{s|p-p'} \frac{1-\beta^2}{|P(p)|} \sum_{q \in P(p)} \Theta_{\infty}^{(L-1; q, q + \frac{p'-p}{s})}(x, y) R_{\dot{\sigma}} \left( \Sigma^{(L-1; q, q + \frac{p'-p}{s})}(x, y) \right) \\ &\geq S^{-L-1/2} (1 - 2(1-\beta^2)r^k) + \delta_{s|p-p'} \frac{1}{|P(p)|} \sum_{q \in P(p)} \Theta_{\infty}^{(L; q, q + \frac{p'-p}{s})}(x, y) (r - \psi 2(1-\beta^2)^2 r^{k-1})\end{aligned}$$

unrolling, we get

$$\begin{aligned}\Theta_{pp'}^{(L)}(x, y) &\geq \sum_{m=0}^k S^{-\frac{L-k+m}{2}} (1 - 2(1-\beta^2)r^m) \prod_{n=m+1}^k (r - \psi 2(1-\beta^2)^2 r^{n-1}) \\ &\geq \sum_{m=0}^k S^{\frac{k-m-L}{2}} r^{k-m} - S^{\frac{k-m-L}{2}} 2(1-\beta^2)r^{k-m} r^m - S^{\frac{k-m-L}{2}} \psi 2(1-\beta^2)^2 \sum_{n=m+1}^k r^{k-m-1} r^{n-1} \\ &\geq S^{-L/2} \frac{1 - (\sqrt{S}r)^{k+1}}{1 - \sqrt{S}r} - 2 \frac{1-\beta^2}{1 - S^{-1/2}} S^{\frac{k-L}{2}} r^k - \psi 2(1-\beta^2)^2 r^{k-1} \sum_{m=0}^k S^{\frac{k-m-L}{2}} \sum_{n=0}^{k-m-1} r^n \\ &\geq S^{-L/2} \frac{1 - (\sqrt{S}r)^{k+1}}{1 - \sqrt{S}r} - 2 \frac{1-\beta^2}{1 - S^{-1/2}} S^{\frac{k-L}{2}} r^k - \psi 2(1-\beta^2)^2 r^{k-1} S^{\frac{k-L}{2}} \frac{1}{1 - S^{-1/2}} \frac{1}{1-r} \\ &\geq S^{-L/2} \frac{1 - (\sqrt{S}r)^{k+1}}{1 - \sqrt{S}r} - 2 \frac{1-\beta^2}{1 - S^{-1/2}} \left[ 1 + \frac{\psi r(1-\beta^2)}{1-r} \right] r^k S^{\frac{k-L}{2}} \\ &\geq S^{-L/2} \left( \frac{1 - (\sqrt{S}r)^{k+1}}{1 - \sqrt{S}r} - C_{\sigma, \beta} (\sqrt{S}r)^k \right)\end{aligned}$$

and for the upper bound:

$$\Theta_{pp'}^{(L)}(x, y) \leq \sum_{m=0}^k S^{-\frac{L-k+m}{2}} \prod_{n=m+1}^k r = S^{-L/2} \frac{1 - (\sqrt{S}r)^{k+1}}{1 - \sqrt{S}r}.$$

Dividing by  $\Theta_{pp}^{(L)}(x, x)$  we obtain

$$\frac{1 - (\sqrt{S}r)^{k+1}}{1 - (\sqrt{S}r)^L} \geq \Theta_{pp'}^{(L)}(x, y) \geq \frac{1 - (\sqrt{S}r)^{k+1}}{1 - (\sqrt{S}r)^L} - \frac{C_{\sigma, \beta} (\sqrt{S}r)^k}{|1 - (\sqrt{S}r)^L|}$$

□

## G Border Effects

With the usual scaling of  $\frac{1}{\sqrt{|\omega|/s_1 \dots s_d}}$ , in a General ConvNet, as defined in Section 2.2, the positions on the border have less parents and hence a lower activation variance. In this section, we show, in a special example, how this parametrization leads to border effects in the limiting activation kernels and NTK. This could be generalized to a more general setting, yet, our main purpose is to show that with the parent-based parametrization—as defined in Section E—no border artifact is present in both kernels in this general setting.

The following proposition illustrates the border artifact present in the usual NTK-parametrization. Let us consider a DC-NN with a standardized ReLU non-linearity, with  $I_0 = I_1 \dots = \mathbb{N}$ , with up-sampling stride of 2, and windows  $\pi_0 = \omega_0 = \pi_1 = \omega_1 = \dots = \{-3, -2, -1, 0\}$ . In particular, there is only one border at position 0. Using the formalism of Section E, the set of parents of a position  $p$  is  $P(p) = \{\lfloor p/2 \rfloor - 1, \lfloor p/2 \rfloor\} \cap \mathbb{N}$ . In particular, any generic position in any hidden or last layer has 2 parents except for the border  $p = 0$  for which  $P(0) = \{0\}$ .

**Proposition 8.** *In the setting introduced above, for any  $x \in \mathbb{S}_{n_0}^{I_0}$ , the kernels satisfy:*

$$\Sigma_{00}^{(\ell)}(x, x) = \frac{\beta^2 + (r/2)^{\ell+1}}{1 - r/2} \text{ and } \Theta_{\infty,00}^{(L)}(x, x) = \frac{\beta^2(1 - (r/2)^L)}{(1 - r/2)^2} + L \frac{(r/2)^{L+1}}{1 - r/2}.$$

*In particular  $\Sigma_{00}^{(\ell)}(x, x)$  is smaller than the “bulk-value”  $\lim_{p \rightarrow \infty} \Sigma_{pp}^{(\ell)}(x, x) = 1$  and  $\Theta_{\infty,00}^{(L)}(x, x)$  is smaller than the “bulk-value”  $\lim_{p \rightarrow \infty} \Theta_{\infty,pp}^{(L)}(x, x) = \frac{1-r^L}{1-r}$ .*

*Proof.* Recall that for the standardized ReLU,  $r_{\sigma,\beta} = 1 - \beta^2$ . From now on, we denote  $r = r_{\sigma,\beta}$  and  $x$  is an element of  $\mathbb{S}_{n_0}^{I_0}$ . For any  $\ell = 0, 1 \dots$ , we have:

$$\Sigma_{00}^{(\ell+1)}(x, x) = \beta^2 + \frac{1 - \beta^2}{2} \sum_{q \in P(0)} \mathbb{E}_{z \sim \mathcal{N}(0, \Sigma_{qq}^{(\ell)}(x, x))} [\sigma(x)^2] = \beta^2 + \frac{1 - \beta^2}{2} \Sigma_{00}^{(\ell)}(x, x).$$

Since  $x \in \mathbb{S}_{n_0}^{I_0}$ , we get  $\Sigma_{00}^{(1)}(x, x) = \beta^2 + \frac{r}{2}$ : this implies the following equalities:

$$\begin{aligned} \Sigma_{00}^{(\ell)}(x, x) &= (r/2)^\ell + \sum_{k=0}^{\ell-1} \beta^2 (r/2)^k \\ &= (r/2)^\ell + \beta^2 \frac{1 - (r/2)^\ell}{1 - r/2} \\ &= \frac{\beta^2}{1 - r/2} + \frac{(r/2)^\ell - (r/2)^{\ell+1} - \beta^2 (r/2)^\ell}{1 - r/2} \\ &= \frac{\beta^2 + (r/2)^{\ell+1}}{1 - r/2}. \end{aligned}$$

For the limiting NTK, with the usual NTK parametrization, the following recursion holds:

$$\Theta_{\infty,00}^{(L+1)}(x, x) = \Sigma_{00}^{(L+1)}(x, x) + \frac{r}{2} \Theta_{\infty,00}^{(L)}(x, x) \mathbb{L}_{\Sigma_{00}^{(L)}}^{\dot{\sigma}}(x, x).$$

Note that for the standardized ReLU,  $\dot{\sigma}$  is a rescaled Heaviside, thus  $\mathbb{L}_{\Sigma_{00}^{(L)}}^{\dot{\sigma}}(x, x) = \mathbb{E}_{x \sim \mathcal{N}(0, \Sigma_{00}^{(L)}(x, x))} [\dot{\sigma}(x)^2] = 2\mathbb{E}_{x \sim \mathcal{N}(0,1)} [\mathbb{I}_{x \geq 0}] = 1$ . This implies:

$$\begin{aligned} \Theta_{00}^{(L)}(x, x) &= \sum_{\ell=1}^L \Sigma_{00}^{(\ell)}(x, x) (r/2)^{L-\ell} \\ &= \sum_{\ell=1}^L \left( \frac{\beta^2}{1 - r/2} + \frac{(r/2)^{\ell+1}}{1 - r/2} \right) (r/2)^{L-\ell} \\ &= \frac{\beta^2}{1 - r/2} \sum_{\ell=1}^L (r/2)^{L-\ell} + L \frac{(r/2)^{L+1}}{1 - r/2} \\ &= \frac{\beta^2(1 - (r/2)^L)}{(1 - r/2)^2} + L \frac{(r/2)^{L+1}}{1 - r/2}. \end{aligned}$$

The “bulk-values” for the activation kernels and the limiting NTK kernel can be deduced from the proof of Proposition 2. A tedious study of variation of functions allows to prove the assertion on the boundary/bulk comparison.  $\square$

As a consequence of the previous proposition, in the limits as  $\ell$  and  $L$  goes to infinity, the ratio boundary/bulk value is bounded by  $\max(1, c\beta^2)$ : the smaller  $\beta$  is, the stronger the boundary effect will be.

In the parent-based parametrization, the variance of the neurons throughout the network is always equal to 1 and the NTK  $\Theta_{\infty,pp}^{(L)}(x, x)$  becomes independent of the position  $p$ : the border artifacts disappear.



**Proposition 2.** For the parent-based parametrization of DC-NNs, if the non-linearity is standardized,  $(\Sigma^{(L)})_{pp}(x)$  and  $(\Theta_{\infty}^{(L)})_{pp}(x)$  do not depend neither on  $p \in I_L$  nor on  $x \in \mathbb{S}_{n_0}^{I_0}$ .

*Proof.* Actually, we will prove the stronger statement: for any General Convolutional Network, as defined in Section E, for any standardized non-linearity, for any  $x \in \mathbb{S}_{n_0}^{I_0}$  and any  $p \in I_L$ ,

$$\Sigma_{pp}^{(L)}(x, x) = 1, \quad \text{and } \Theta_{\infty, pp}^{(L)}(x, x) = \frac{1 - r^L}{1 - r}.$$

For the activation kernels, this is proven by induction on  $\ell$ . For any  $x \in \mathbb{S}_{n_0}^{I_0}$  and any  $p \in I_1$ :

$$\begin{aligned} \Sigma_{pp}^{(1)}(x, x) &= \beta^2 + \frac{1 - \beta^2}{|P(p)| n_0} \sum_{q \in P(p)} \sum_{q' \in P(p)} \chi(q \rightarrow p, q' \rightarrow p) x_q^T x_{q'} \\ &= \beta^2 + \frac{1 - \beta^2}{|P(p)| n_0} \sum_{q \in P(p)} x_q^T x_q \\ &= \beta^2 + (1 - \beta^2) \\ &= 1, \end{aligned}$$

and if the assertion holds true for  $L$ , then:

$$\begin{aligned} \Sigma_{pp}^{(L+1)}(x, x) &= \beta^2 + \frac{1 - \beta^2}{|P(p)| n_0} \sum_{q \in P(p)} \sum_{q' \in P(p)} \chi(q \rightarrow p, q' \rightarrow p) \Sigma_{qq'}^{(L)}(x, x) \\ &= \beta^2 + \frac{1 - \beta^2}{|P(p)| n_0} \sum_{q \in P(p)} \Sigma_{qq}^{(L)}(x, x) \\ &= 1. \end{aligned}$$

For the activation kernels, this is proven by induction on  $L$ . It is easy to see that  $\Theta_{\infty, pp}^{(1)}(x, x) = 1$  is valid for any  $x \in \mathbb{S}_{n_0}^{I_0}$  and any  $p \in I_L$ . Let us show the induction step:

$$\begin{aligned} \Theta_{\infty, pp}^{(L+1)}(x, x) &= \Sigma^{(L+1, pp)}(x, x) + \frac{1 - \beta^2}{|P(p)|} \sum_{q \in P(p)} \Theta_{\infty, qq}^{(L)}(x, x) R_{\sigma} \left( \Sigma_{qq}^{(L)}(x, x) \right) \\ &= 1 + r \Theta_{\infty, qq}^{(L)}(x, x). \end{aligned}$$

Thus,  $\Theta_{\infty, pp}^{(L)}(x, x) = \sum_{\ell=1}^L r^{L-\ell} = \frac{1-r^L}{1-r}$ .  $\square$

## H Layerwise Contributions to the NTK and Checkerboard Patterns

In a DC-NN with stride  $s \in \{2, 3, \dots\}^d$ , if two connection weight matrices  $W^{(\ell, q \rightarrow p)}$  and  $W^{(\ell, q' \rightarrow p')}$  are shared then  $s \mid p' - p$ . In other words,  $\chi(q \rightarrow p, q' \rightarrow p') = 0$  as soon as  $s \nmid p' - p$ . The limiting contribution of the weights  $\Theta_{\infty}^{(L:W^{(\ell)})}$  and bias  $\Theta_{\infty}^{(L:b^{(\ell)})}$  to the limiting NTK can be formulated recursively. For the last layer  $L - 1$  we have

$$\begin{aligned} \Theta_{\infty, pp'}^{(L:b^{(L-1)})} &= \beta^2 \\ \Theta_{\infty, pp'}^{(1:W^{(0)})} &= \delta_{s \mid p-p'} \frac{1 - \beta^2}{|P(p)| n_0} \sum_{q \in P(p)} x_q^T y_{q + \frac{p'-p}{s}} \\ \Theta_{\infty, pp'}^{(L:W^{(L-1)})} &= \delta_{s \mid p-p'} \frac{1 - \beta^2}{|P(p)|} \sum_{q \in P(p)} R_{\sigma} \left( \Sigma_{q, q + \frac{p'-p}{s}}^{(L-1)}(x, y) \right) \text{ for } L > 1 \end{aligned}$$

and for the other layers, we have

$$\begin{aligned}\Theta_{\infty, pp'}^{(L+1; b^{(\ell)})} &= \delta_{s|p-p'} \frac{1-\beta^2}{|P(p)|} \sum_{q \in P(p)} \Theta_{\infty, q, q+\frac{p'-p}{s}}^{(L; b^{(\ell)})}(x, y) R_{\dot{\sigma}} \left( \Sigma_{q, q+\frac{p'-p}{s}}^{(L)}(x, y) \right) \\ \Theta_{\infty, pp'}^{(L+1; W^{(\ell)})} &= \delta_{s|p-p'} \frac{1-\beta^2}{|P(p)|} \sum_{q \in P(p)} \Theta_{\infty, q, q+\frac{p'-p}{s}}^{(L; W^{(\ell)})}(x, y) R_{\dot{\sigma}} \left( \Sigma_{q, q+\frac{p'-p}{s}}^{(L)}(x, y) \right).\end{aligned}$$

**Proposition 3.** *In a DC-NN with stride  $s \in \{2, 3, \dots\}^d$ , we have  $\Theta_{\infty, pp'}^{(L; W^{(\ell)})}(x, y) = 0$  if  $s^{L-\ell} \nmid p' - p$  and  $\Theta_{\infty, pp'}^{(L; b^{(\ell)})}(x, y) = 0$  if  $s^{L-\ell-1} \nmid p' - p$ .*

*Proof.* From the formulas of the limiting contributions  $\Theta^{(L; W^{(\ell)})}$  and  $\Theta^{(L; b^{(\ell)})}$ , we see that the bias of the last layer contribute to all pairs  $p, p'$  while the bias only contribute to pairs such that  $s \mid p' - p$ . Now by induction on  $L$ , if  $\Theta_{qq'}^{(L; b^{(\ell)})}$  and  $\Theta_{qq'}^{(L; W^{(\ell)})}$  only contribute to pairs  $q, q'$  such that  $s^{L-\ell-1} \mid q' - q$  and  $s^{L-\ell} \mid q' - q$  then

$$\begin{aligned}\Theta_{\infty, pp'}^{(L+1; b^{(\ell)})} &= \delta_{s|p-p'} \frac{1-\beta^2}{|P(p)|} \sum_{q \in P(p)} \Theta_{\infty, q, q+\frac{p'-p}{s}}^{(L; b^{(\ell)})}(x, y) R_{\dot{\sigma}} \left( \Sigma_{q, q+\frac{p'-p}{s}}^{(L)}(x, y) \right) \\ \Theta_{\infty, pp'}^{(L+1; W^{(\ell)})} &= \delta_{s|p-p'} \frac{1-\beta^2}{|P(p)|} \sum_{q \in P(p)} \Theta_{\infty, q, q+\frac{p'-p}{s}}^{(L; W^{(\ell)})}(x, y) R_{\dot{\sigma}} \left( \Sigma_{q, q+\frac{p'-p}{s}}^{(L)}(x, y) \right)\end{aligned}$$

only contribute to pairs  $p', p$  such that  $s^{L-\ell} \mid p' - p$  and  $s^{L+1-\ell} \mid p' - p$  as needed.  $\square$